Network Analysis of Rare Single-Nucleotide Polymorphisms Suggests a Central Role for Type 17 Immune Responses in Trauma-induced, Genotypically Associated Hypo-Inflammation and Critical Illness

Fayten El-Dehaibi[1,*], Ruben Zamora[1,*], Jinling Yin[1], Timothy R. Billiar[1], Yoram Vodovotz[1,2,†]

Running Title: Trauma-associated SNPs and Th17 Inflammation

[1]Department of Surgery, University of Pittsburgh, Pittsburgh, PA 15213

[2] Center for Inflammation and Regeneration Modeling, McGowan Institute for Regenerative Medicine, University of Pittsburgh, Pittsburgh, PA 15219

[*]Co-first authors

[†] **To whom correspondence should be addressed at**:
Department of Surgery
University of Pittsburgh
W944 Starzl Biomedical Sciences Tower
200 Lothrop St.
Pittsburgh, PA 15213
Tel.: 412-647-5609
Fax: 412-383-5946
E-mail: vodovotzy@upmc.edu

Keywords: trauma, SNP, Th17, hypo-inflammation, RORA

Word Count: 4959 words

Figure Count: 13 (11 figures, 2 tables)

Printed on October 6, 2025

ABSTRACT

Critical illness stemming from severe traumatic injury is a leading cause of morbidity and mortality worldwide, involves the dysfunction of multiple organ systems, and is driven at least in part by dysregulated inflammation that involves type 17 immunity. We and others have demonstrated a genetic predisposition to adverse critical illness outcomes associated with single-nucleotide polymorphisms (SNPs) in novel loci distinct from those which impact type 17 immune responses yet acting in concert with those responses. We have recently developed *SNPScanner*, an algorithm that enables rapid scanning through a large SNP dataset and associated inflammation biomarkers and clinical data, and in the present study leveraged this algorithm in concert with existing bioinformatics tools to define networks of interaction among rare SNPs (defined operationally as being present in 5-10% of patients due to the study cohort size) assessed in critically ill trauma patients. RAR-related orphan receptor A (RORA), a transcription factor central to the differentiation of Th17 cells, was inferred as a hub gene via its SNP rs4774381; stratification of trauma patients based on homozygous genotype at this SNP pointed to distinct organ dysfunction trajectories associated with network-defined hypo-inflammation. Further, the SNP rs11919443 in the non-hub *TM4SF19* gene distinguished genotype-associated systemic IL-17A trajectories, and associated hypo-inflammation with adverse outcomes. In contrast, no Th17-related hub genes were identified in a control group of SNPs associated algorithmically with adverse clinical outcomes but with genotypically indistinct systemic inflammatory responses; the main inferred hub gene in this control group was solute carrier family 2, facilitated glucose transporter member 1 (*SLC2A1*)/glucose transporter 1 (GLUT1). Secondary analysis showed several statistically significant differences in circulating inflammatory mediators not including IL-17A, and also associated network-based hypo-inflammation with adverse outcomes in this control group. This study thus extends our prior work aimed at defining genetic predisposition to dysregulated inflammation and pathophysiology in the context of critical illness, and points to a crucial role for type 17 immune responses.

1. INTRODUCTION

Trauma-induced critical illness, in which organ dysfunction is associated with dysregulated inflammation (i.e., an abnormal or imbalanced immune response with detrimental effects to the body), represents a major global health burden (1-3). Despite similar injury profiles and demographics, and the use of standardized protocols, critically ill trauma patients exhibit heterogeneous outcomes (4). We and others have proposed that genetic variation among patients may account for some of this heterogeneity (5). Previous studies have identified distinct dynamic inflammatory networks after severe trauma as a function of demographics (e.g., age) (6), injury timing (7) and characteristics (8-11), or clinical outcomes (12, 13). We have also characterized endotypes of blunt trauma patients based on early inflammatory patterns (14, 15), multiple organ dysfunction severity (16), or multi-'omics patterns (17, 18). A key immune pathway that emerged from these studies involves interleukin-17A (IL-17A), suggesting a novel, early role for type 17 immune responses in trauma-associated critical illness (13, 15, 19-21).

Our studies have also highlighted a role for genetic polymorphisms in the disordered systemic inflammation that is characteristic of critically ill trauma patients (19, 22-25). These studies, particularly those showing that specific single-nucleotide polymorphisms (SNPs) are linked to sub-acute mortality in trauma patients with early divergent inflammatory trajectories associated with the Multiple Organ Dysfunction Syndrome (MODS) (13, 24), imply that genetic factors may influence the variability in patient outcomes and acute inflammation in critically ill trauma patients.

We have previously developed novel computational approaches to aid in the search for novel, yet common (defined as present in 20% or more of the patients in our study cohort) SNPs associated with altered trajectories of systemic inflammation and subsequent clinical outcomes (24), and have combined this discovery program with existing computational tools that facilitate the discovery of SNPs in networks of genes acting in concert (25). In the present study, we leveraged these two approaches to scan a dataset of >500,000 SNPs for networks of both rare and common SNPs associated with adverse outcomes in critically ill trauma patients. In these analyses, we focused on defining hub genes and assessing clinical outcomes and inflammatory profiles in patient subgroups stratified based on genotypes at those hub genes. Our results suggest a key role for Th17 differentiation and associate this with systemic hypo-inflammation.

2. MATERIALS AND METHODS

2.1 *Trauma patient cohort*

Studies were carried out using a cohort of 380 blunt trauma survivors with roughly equivalent distributions of homozygous and alternative homozygous genotypes at any of >500,000 SNPs described previously (24). In brief, patients were enrolled by screening after presentation to the emergency department of the UPMC Presbyterian hospital (a Level 1 trauma center) between May 5, 2004, to May 2, 2012. Patients eligible for enrollment in the study were at least 18 years of age, admitted to the intensive care unit (ICU) after being resuscitated, and, per treating physician, were expected to live more than 24h. Exclusion criteria were isolated head injury, pregnancy, and penetrating trauma. Informed consent was obtained from each patient or next of kin as per the University of Pittsburgh Institutional Review Board (IRB; Protocol No. MOD08010232-19 / PRO08010232) and in accordance with the Declaration of Helsinki. Blood samples for DNA and inflammatory biomarker analysis were obtained upon admission to the trauma bay, at first 24 h of hospitalization, and daily thereafter for 7 days.

Clinical data, including injury severity score (ISS), abbreviated injury scale (AIS) score, Marshall Multiple Organ Dysfunction (MOD) score, admission Shock Index, ICU LOS, hospital LOS, and days on mechanical ventilation were collected from the hospital inpatient electronic and trauma registry database. ISS (26) and AIS (27) were calculated for each patient by a single trauma surgeon after attending radiology evaluations were finalized. The ISS is based on an anatomical scoring system that provides an overall score for patients with multiple injuries. Each injury is assigned an AIS score, allocated to one of six body regions: head, face, chest, abdomen, extremities (including pelvis), and external. As an index of organ dysfunction, the MOD score (28) ranging from 0 to 24 was calculated. In brief, six variables were obtained from the electronic trauma data registry including (a) the respiratory system (PO_2/FIO_2 ratio); (b) the renal system (serum creatinine concentration); (c) the hepatic system (serum bilirubin concentration); (d) the hematologic system (platelet count); (e) the central nervous system (Glasgow Coma Scale); and (f) the cardiovascular system- the pressure-adjusted heart rate (PAR).

The overall characteristics of the patients in the trauma cohort were as follows (mean ± SD): (ISS) = 19.0 ± 10.1 [min: 1; max: 54]; mean age: 49.3 ± 19.2 years (min: 18y; max: 90y); 119 women, 261 men; 96.84% whites, 2.63% blacks and 0.53% others.

2.2 *Genomic analyses*

For the blunt trauma patient cohorts, DNA was prepared from whole blood samples and analyzed using Illumina® arrays as described previously (19, 22, 23). Whole blood samples were collected into EDTA-treated tubes and DNA was extracted using the QIAamp® DNA Blood Midi Kit (QIAGEN, Valencia, CA) as per manufacturer's specifications. Single nucleotide polymorphism genotyping was performed with 200 ng of genomic DNA input using the Human Core Exome-24 v1.1 BeadChip (Illumina, San Diego, CA) following the manufacturer's Infinium® HTS Assay protocol. This array interrogated 551,839 SNPs, including both SNPs previously implicated in genome-wide association studies as well as additional coding and non-coding SNPs spaced along the human genome. Briefly, DNA was denatured in 0.1N NaOH and neutralized prior to isothermal amplification. Amplified DNA was fragmented and then hybridized to locus-specific 50mers that make up the array for 16-24 h with rocking at 48˚C. After removal of unbound or non-specifically annealed DNA, single base extension of the 50mer

135 oligonucleotides was performed with labeled nucleotides, which were scanned using an Illumina
136 iScan with autoloader 2.x. Data analysis was performed using Illumina Genome Studio 2.0.
137
138 **2.3 *Assays of inflammation biomarkers***
139 Whole-blood samples were drawn in EDTA-treated tubes, which were kept on ice and
140 centrifuged to obtain plasma and then stored at -80°C until assays were performed. The
141 Luminex™ 100 IS analyzer (Luminex, Austin, TX) and Human Cytokine/Chemokine
142 MILLIPLEX™ Panel kit (Millipore Corporation, Billerica, MA) were used to measure plasma
143 levels of Eotaxin (CCL11), interleukin (IL)-1β, IL-1 receptor antagonist (IL-1RA), IL-2, soluble
144 IL-2 receptor-α (sIL-2Rα), IL-4, IL-5, IL-6, IL-7, IL-8 (CCL8), IL-10, IL-13, IL-15, IL-17A,
145 interferon (IFN)-α, IFN-γ, IFN-γ inducible protein (IP)-10 (CXCL10), monokine induced by
146 gamma interferon (MIG; CXCL9), macrophage inflammatory protein (MIP)-1α (CCL3), MIP-1β
147 (CCL4), monocyte chemotactic protein (MCP)-1 (CCL2), granulocyte-macrophage colony
148 stimulating factor (GM-CSF) and tumor necrosis factor alpha (TNF-α). Human Th17
149 MILLIPLEX™ Panel kit (Millipore Corporation, Billerica, MA) was used to measure IL-9, IL-
150 21, IL-22, IL-23, IL-17E/25, and IL-33. NO2-/NO3 levels were measured by a Griess Reagent
151 colorimetric assay (Cayman Chemical, Ann Arbor, MI). IL-1 receptor-like 1/ suppression of
152 tumorigenicity-2 (ST2) was measured by a sandwich ELISA assay (R&D Systems, Minneapolis,
153 MN). All cytokine/chemokine concentrations are given in pg/ml; NO2-/NO3- concentrations are
154 in μM. Experimental data are shown as mean ± SEM.
155
156 **2.4 *FLAME and associated bioinformatics analyses***
157 Functional Enrichment Analysis was performed using the web application FLAME (v2.0)
158 (29). Two lists of SNPs— the first associated with trajectories of systemic inflammation typical
159 that did not differ based on genotype (which served as controls) vs. SNPs associated with
160 genotype-specific differential systemic inflammatory responses as determined in our prior study
161 (24) —were separately entered into the SNP tab of the Input page (Table 1). To reduce potential
162 artifacts in this analysis, 15 SNPs associated with 12 or more genotype-specific differential
163 systemic inflammatory responses as determined in our prior study (22) were selected out of 7482
164 SNPs which met the initial criterion of having at least one statistically different biomarker
165 difference as a function of SNP genotype in our original study (22). In the control group for
166 evenly distributed genotypes, SNPs were extracted from the group of 567 SNPs with zero
167 significantly different mediators as a function of genotype at each given SNP (described initially
168 in (22). To decrease the likelihood of artifactual associations among SNPs and to obtain
169 meaningful information about associations of SNPs with inflammation, we imposed an
170 additional condition of having at least 3-4 significant differences in clinical outcomes as a
171 function of SNP genotype which is to find SNPs while having no significant differences in
172 inflammation biomarkers. This led to down-selection from 567 to 16 SNPs.
173 To examine less-common SNPs (referred to as 'rare' for our purposes) we performed the
174 process described to extract differential inflammatory SNPs from the human trauma group but
175 used a 5–10% to 90–95% ratio of homozygous prevalence (minimum 20 patients) to select 7212
176 SNPs from the original >500,000. The previous method was applied to run Mann-Whitney U
177 analysis on the same 30 inflammatory biomarkers on patients from each group. Given the
178 population size disparity between the homozygotes of the rare SNP set, we sought to reduce the

likelihood of artifactual results by considering p-values less than 10-5 as significant, as opposed to 0.05 used earlier. This stringency provided 131 SNPs associated with at least one statistically significant biomarker, and 15 SNPs with up to two. The omission of X-linked SNPs yielded 12 rare somatic SNPs with at least two significantly different inflammatory biomarkers. The rare SNP subset was also checked for control SNPs in the same manner described for the evenly distributed SNPs. Screening clinical outcomes with Mann-Whitney U reduced 433 rare SNPs with zero significantly different mediators ($p < 0.05$) down to 10 with at least 3-4 statistically different outcomes.

Each list of corresponding genes found was separately inputted into FLAME's Functional Enrichment page for whole genome search, with the enrichment tools set to gProfiler (30) and enrichR (31) and the significance threshold set to 0.05. The following data sources were selected: Molecular Function, Cellular Component and Biological Function from the gene ontology knowledgebase (GO)(32), and the Kyoto Encyclopedia of Genes and Genomics (KEGG) (33).

2.5 *Statistical analyses*

Kruskal-Wallis Analysis of Variance (ANOVA) on Ranks, One-Way and Two-Way ANOVAs were conducted to analyze the differences in ISS, AIS, Marshall MODScore, and time-dependent changes in plasma biomarkers in AA and BB patients using SigmaPlot (Systat Software, San Jose, CA) as appropriate. Two-Way ANOVA was followed by the Holm-Sidak *post hoc* test to isolate which group(s) differ from the others. Chi-square analysis of the proportions of observations for patients with rs10404939 or rs11117564 genotype was performed using SigmaPlot (Systat Software, San Jose, CA).

2.6 *Network analysis*

Dynamic Network Analysis (DyNA) was carried out to define, in a granular fashion, the central inflammatory network nodes as a function of both time and patient subgroup. DyNA networks were created over six consecutive time periods (D1-D2, D2-D3, D3-D4, D4-D5, D5-D6, D6-D7) using MATLAB® software as described previously(34-36). Connections, defined as the number of inflammatory biomarkers that were positively or negatively correlated across time intervals, were created if the Pearson correlation coefficient between any two nodes (biomarkers) at the same time-interval was greater or equal to a threshold of an absolute value of 0.95, as appropriate. The network complexity for each time-interval was calculated using the following formula: Sum $(N_1 + N_2 + \ldots + Nn)/(n - 1)$, where N represents the number of connections for each biomarker and n is the total number of biomarkers analyzed.

2.7 *Th17 Cell Subset Inference/Correlation Analysis*

Spearman's correlation carried out to measure the strength of the association between the Luminex™ data for two different mediators (IL-17A and each of the following: GM-CSF, IL-10, TNF-α, and IL-22) was generated using MATLAB® software (Natick, MA).

3. RESULTS

3.1 Bioinformatic analysis defines networks of interaction among rare SNPs in blunt trauma patients and implicates Th17 differentiation and systemic hypo-inflammation. We have previously searched for common SNPs (defined operationally as being present in 20% or more of our study cohort) that might be both unlikely and associated with dysregulated inflammation and adverse clinical outcomes in the context of critical illness, and found one such SNP in the *LYPD4* gene (out of >500,000 assessed SNPs) using a Python-based algorithm we term *SNPScanner* (24).

In the present study, we sought to study less common SNPs and focused on SNPs present in 5-10% of the population to allow for a sufficient number of patients in the various comparison groups. Herein, we refer to these SNPs as "rare" to distinguish them from the "common" *LYPD4* SNP identified previously (24), acknowledging that most SNPs are found in between 0.5 and 5% of the global population, and SNPs found in a greater proportion of individuals are unlikely (37). Our search yielded 12 somatic SNPs associated with two highly statistically significantly different inflammation biomarkers (based on the initial Mann-Whitney U-test performed in the *SNPScanner* algorithm), with a p-value < 0.00001 between subgroups of patients homozygous for the main allele at a given SNP (referred to as AA) vs. the alternative homozygous allele at that SNP (referred to as BB). We then carried out Functional Enrichment Analysis using the web application FLAME (29). When the *SNPScanner* results were entered into FLAME, one of these SNPs, three major and one minor hub gene were identified.

One major hub gene, with three connections, was identified via the SNP rs4774381 in the gene encoding RAR-related orphan receptor A (RORA), which is involved in Th17 differentiation (38) (Figure 1). When segregating trauma patients based on AA vs. BB genotype at this SNP, statistically significant differences were noted in circulating IL-17A along with IFN-γ, IL-1RA, IL-5, IL-7, IL-10, MIG/CXCL9, sIL-2rα, and sST2 (Figure 2A). This was associated with statistically significant differences in MODS trajectories (Figure 2B) but not in admission Shock Index between AA and BB ($p=0.799$). Paradoxically, $rs4774381^{AA}$ exhibited significantly ($p < 0.001$) lower Marshall MODScores as compared to $rs4774381^{BB}$ patients despite the elevated systemic inflammation in $rs4774381^{AA}$ vs. $rs4774381^{BB}$ patients (Figure 2B). This finding raised the possibility that pathological hypo-inflammation might be associated with adverse outcomes, as suggested in our prior work (15). In support of this hypothesis, we note the early elevation of systemic IL-10, a key anti-inflammatory cytokine, in $rs4774381^{BB}$ patients as compared to $rs4774381^{AA}$ patients.

We next utilized Dynamic Network Analysis (DyNA) (39) to define networks of interaction among all systemic inflammatory mediators in $rs4774381^{AA}$ vs. $rs4774381^{BB}$ patients (Figure 3). This analysis demonstrated striking differences in network patterns between these two patient subgroups. Specifically, the dynamic networks of systemic inflammation inferred in $rs4774381^{AA}$ (Figure 3A, 3C) were much sparser at early time points post-hospitalization than those inferred in $s4774381^{BB}$ patients (Figure 3B, 3C). In addition, both $rs4774381^{AA}$ and $rs4774381^{BB}$ patients exhibited oscillating systemic inflammation networks over the first seven days following hospitalization, with the amplitude of oscillation appearing to manifest a "phase shift" when comparing the two patient subgroups (Figure 3C).

The overall network connectivity difference between homozygous subgroups was also reflected in the network connectivity of individual inflammatory mediators (Figure 3D). Multiple

262 inflammatory mediators that had zero connections in networks inferred in rs4774381^{AA} patients
263 exhibited high connectivity in rs4774381^{BB} patients; this included IL-17A as well as IL-5, GM-
264 CSF, sIL-2rα, and IL-6 (Figure 3D). In contrast, Eotaxin and IFN-α exhibited the opposite
265 pattern, with zero network connections inferred in rs4774381^{BB} patients and high connectivity in
266 rs4774381^{AA} patients (Figure 3D). Overall, the most connected mediators were MIP-1β and IL-2,
267 both inferred in rs4774381^{BB} patients (Figure 3D).
268 Since RORA is a key transcription factor associated with Th17 differentiation (38), we
269 next carried out a correlation analysis aimed at inferring Th17 cell subsets as in prior studies (13,
270 15, 19), noting that identification of Th17 cells in trauma patients using this correlation-based
271 analysis was supported by more direct methods in studies carried out by others (40). This
272 analysis involves correlation of circulating IL-17A with circulating GM-CSF, IL-10, TNF-α, and
273 IL-22 to infer the presence of pathogenic Th17 cells (IL-17A vs. GM-CSF), non-pathogenic
274 Th17 cells (IL-17A vs. IL-10), memory/effector T cells (IL-17A vs. TNF-α), and δγ T cells (IL-
275 17A vs. IL-22), respectively (Figure 4), and suggested distinct patterns of Th17 subpopulations
276 based on statistically significant inter-mediator correlations. Specifically, we found a significant
277 correlation between IL-17A and IL-10 only in rs4774381^{AA} patients (compare Figure 4B and
278 4F), suggesting the predominance of non-pathogenic (non-inflammatory (38)) Th17 cells in these
279 patients. Both rs4774381^{AA} and rs4774381^{BB} patients exhibited statistically significant
280 correlations between IL-17A and TNF-α (compare Figures 4C and 4G) as well as IL-22
281 (compare Figures 4D and 4H), suggesting similar levels of memory/effector and δγ T cell
282 responses, respectively. Finally, neither patient subgroup exhibited an upregulation of pathogenic
283 Th17 cells as inferred from non-significant correlations between IL-17A and GM-CSF (compare
284 Figures 4A and 4E). This analysis suggests that upregulation of non-pathogenic Th17 cells is
285 associated with hypo-inflammation following severe injury.
286 The SNP rs7918717 in the *RPP38* gene, which codes for a subunit of RNAse P (41) was
287 the second major hub gene identified by FLAME, with four connections. Interestingly, the SNP
288 rs7918717 in the *NMT2* gene was identified as a minor hub gene with one connection also to
289 rs7918717. Patients stratified based on genotype (AA vs. BB) at this SNP exhibited significantly
290 different circulating GM-CSF ($p=0.014$) as well as MODS trajectories ($p=0.024$), but not in ICU
291 LOS, total LOS, days on mechanical ventilation, ISS, and AIS ($p>0.05$, not shown). There was
292 no statistically significant difference in Shock Index between AA and BB ($p=0.866$).
293 The SNP rs261537 in the *UBE2D2* gene was the third major hub gene identified by
294 FLAME, with 2 connections. The AA and BB subgroups at this SNP exhibited statistically
295 significant differences in both circulating IFN-γ ($p=0.026$) and GM-CSF ($p=0.042$). However,
296 we found no significant differences in any of the clinical characteristics analyzed (not shown).
297
298 **3.2 rs11919443 in the *TM4SF19* gene is associated with distinct trajectories of multiple**
299 **systemic inflammatory mediators including IL-17A and hypo-inflammation, but not with**
300 **distinct Th17 cell subsets.** We next hypothesized the trauma patient subgroups segregated based
301 on non-hub, rare SNPs associated with genotypically distinct systemic inflammation profiles
302 would also exhibit differences in circulating IL-17A. One such SNP was rs11919443 in the gene
303 coding for transmembrane 4 L six family member 19 (*TM4SF19*). In support of this hypothesis,
304 rs11919443^{AA} patients exhibited significantly elevated levels of circulating IL-17A as compared
305 to rs11919443^{BB} patients (Figure 5A). In addition, the following circulating inflammatory

306 mediators were also significantly different between the two groups by Two-Way ANOVA: IL-6
307 (p=0.005), IL-7 (p=0.007), IL-8 (p=0.001), IL-10 (p=0.017), MCP-1 (p<0.001) and sST2
308 (p<0.001). These differences were associated with significantly different clinical outcomes,
309 including longer ICU stay (Figure 5C) and longer time on mechanical ventilation (Figure 5D) in
310 rs11919443^{AA} patients as compared to rs11919443^{BB} patients. In contrast, there was no
311 statistically significant difference in Shock Index between AA and BB (p=0.207),
312 Similarly to the analysis of patients stratified based on genotype at rs4774381, inference
313 of dynamic networks in rs11919443^{AA} patients as compared to rs11919443^{BB} patients suggested
314 a striking hypo-inflammatory phenotype, with rs11919443^{BB} patients exhibiting zero
315 inflammatory network connectivity while rs11919443^{AA} patients exhibited fairly robustly
316 connected networks (Figure 6A) (Supplementary Figure 2). The most connected mediators (with
317 10 connections or more) in rs11919443^{AA} patients were, in descending order, IL-5, IL-7, IL-2,
318 IL-15, IL-1β, GM-CSF, IL-1RA, IL-17A, IFN-γ, and IFN-α (Figure 6B). In agreement with the
319 less important role of IL-17A in these dynamic networks, and in contrast with the analysis
320 carried out on patients stratified based on homozygous genotype rs4774381 at the hub gene
321 *RORA*, rs11919443 patient subgroups exhibited no major inferred differences in their Th17
322 subsets (Figure 7).
323
324 **3.3 Analysis of SNP networks in a control group defined algorithmically as having**
325 **genotypically associated differences in clinical outcomes but not circulating inflammatory**
326 **mediators implicates *SLC2A1*.** The 443 rare SNPs with zero statistically significant mediators
327 were entered into FLAME, which returned 261 SNP-gene permutations. When we added the
328 requirement that the control SNPs must have 3-4 statistically different post-traumatic outcomes,
329 the number of rare control SNPs fell to 10 SNPs. Running these SNPs through FLAME resulted
330 in five genes associated with a given SNP within the set, of which four gave results for
331 functional enrichment (Supplementary Table 2). The four genes are *SLC2A1* (associated with
332 rs841852), *IQSEC2* (rs1409117), *ABI3BP* (rs7609779), and *RGS21* (rs7514892). Of these, only
333 *SLC2A1* (solute carrier family 2, facilitated glucose transporter member 1/glucose transporter 1
334 [GLUT1]), indicated by its SNP rs841852, was a hub gene (Figure 8A-B). Patients segregated
335 based on their genotype at rs841852 (AA vs. BB) did not differ with regard to injury severity
336 (ISS as well as AIS) and Shock Index (p=0.066) but did exhibit statistically significant
337 differences in (Figure 8C-G): ICU length of stay (p< 0.002), total hospital length of stay (p=
338 0.046), and Marshall MODScore (p< 0.001). Circulating inflammatory mediators in the two
339 genotypes differed significantly (Two-Way ANOVA) in IL-1RA (p= 0.019), IL-7 (p = 0.032),
340 IL-13 (p< 0.001), IL-15 (p= 0.006), MIG (p= 0.024), and sIL-2Ra (p= 0.003) (Figure 9).
341 Similarly to the hypo-inflammation inferred in dynamic networks observed in the other
342 SNP comparison groups, trauma patients segregated based on alternative homozygous genotype
343 at rs841852 exhibited overall low inflammatory network connectivity except in rs841852^{AA}
344 patients at time points from day 4-7 post-hospitalization; rs841852^{BB} patients exhibited zero
345 network connections at all time points (Figure 10A). Mediators with 10 or more connections in
346 rs841852^{AA} patients were, in descending order, MIP-1α, IL-4, IL-5, IFN-γ, IL-7, IL-13, IL-17A,
347 IL-1RA, and IL-33 (Figure 10B; Supplementary Figure 3). Consistent with the hypothesis of
348 hypo-inflammation in rs841852^{BB} patients was a mild inferred upregulation of non-pathogenic

349 Th17 cells while other inferred Th17 subsets were generally similar between patient subgroups
350 (Figure 11).

351 **4. DISCUSSION**

352 The present study extends multiple prior studies linking specific genetic polymorphisms
353 to outcomes of trauma-associated critical illness (19, 22, 23, 25, 42, 43). Specifically, we
354 leveraged novel bioinformatics tools and approaches to implicate the Th17-related RAR-related
355 orphan receptor A (RORA) transcription factor (54) as a major hub gene in networks of SNPs
356 associated with dysregulated systemic inflammation in blunt trauma patients. Segregating blunt
357 trauma survivors based on alternative homozygous genotypes at rs11919443, a non-hub, intronic
358 SNP in the *TM4SF19* gene also identified in this search, yielded subpopulations of patients with
359 distinct trajectories of systemic inflammatory mediators including IL-17A. Furthermore, these
360 subpopulations also differed in key critical illness outcomes but not in core demographics or
361 injury/hemorrhage characteristics, supporting the notion that the differences we identified are
362 due to genetic causes. Our study also suggested *SLC2A1*/*GLUT1* as a hub gene in the responses
363 of trauma patients whose systemic inflammation was not characterized by extensive,
364 genotypically associated differences while still exhibiting genotypically related differences in
365 clinical outcomes. Finally, the present study also highlighted the presence and possible
366 pathophysiologic role of systemic hypo-inflammation, and implicated differential IL-17A
367 production in this process.
368 Interleukin-17A is a pro-inflammatory cytokine that is produced by Th17 cells, innate
369 lymphoid cells, γδ T cells, and natural killer cells among others (44-50). Interleukin-17A and
370 Th17 cells were studied initially in the context of chronic inflammatory/autoimmune diseases
371 such as rheumatoid arthritis, Crohn's disease, psoriasis, and systemic lupus erythematosus (SLE)
372 (49, 51). More recently, this pathway has been implicated in acute inflammatory states such as
373 sepsis (52, 53), trauma/hemorrhagic shock (13, 15, 20), COVID-19 (54), wound healing (55),
374 and acute allograft rejection (56).
375 Interleukin-17A and Th17 cells have also been implicated in the dysregulated
376 inflammation that accompanies adverse outcomes in the context of critical illness, based on
377 initial studies in animal models of sepsis (52, 53) and subsequent studies in human trauma
378 patients (13, 40). Specifically, mortality in trauma-associated critical illness (13) was associated
379 with a predominance of so-called pathogenic Th17 cells (57, 58). In these initial studies
380 documenting an early role for IL-17A in dynamic networks of self-sustaining inflammation, we
381 inferred an upregulation of pathogenic Th17 cells and a concomitant downregulation of
382 nonpathogenic Th17 cells (13). Our initial study associating seven novel SNPs with mortality
383 extended these initial findings and suggested that this genetic predisposition to mortality in the
384 context of trauma-associated critical illness was not determined solely by these SNPs but also
385 required a predominant pathogenic Th17 phenotype that was in turn associated with an overall
386 elevated systemic inflammatory response (19). These results pointed to related, but distinct, roles
387 for genetic predisposition as well as systemic inflammation characterized by distinct Th17
388 subsets, and this was confirmed in subsequent studies (22). In the present study, we extend these
389 results further with the observation that the flip side of pathogenic Th17-driven, self-sustaining
390 hypo-inflammation is a genetically controlled predisposition to hypo-inflammation characterized
391 by an upregulation of non-pathogenic Th17 cells. We note the early upregulation of systemic IL-
392 10 and inferred upregulation of non-pathogenic Th17 cells in rs4774381^{BB} patients as compared
393 to rs4774381^{AA} patients. We have suggested a similar phenotype in patients stratified based on a

394 SNP in the *CD55* gene (25). This hypothesis needs to be tested in larger patient cohorts as well
395 as via mechanistic perturbations in appropriate experimental models.
396 A related hypothesis concerns the IL-10 family cytokine IL-22 (59) and the correlation
397 between IL-17A and IL-22. In this and related studies, we have inferred the presence of γδ T
398 cells based on a positive correlation between IL-17A and IL-22. However, this supposition
399 would need to be tested directly by examining cellular profiles and other markers specific for any
400 of the inferred cell subpopulations, as noted above. It is also possible that the positive correlation
401 between IL-17A and IL-22 reflects an IL-17A-induced upregulation of IL-22 by other cell types.
402 In this regard, recent studies have implicated epithelial-derived IL-22 and related tissue-
403 protective cytokines such as IL-21 and IL-17E/IL-25 in the context of the response to traumatic
404 injury (60). It is intriguing to speculate that IL-17A, derived from any of the cell populations that
405 can produce this cytokine, induces IL-22 from epithelial cells in various tissues and that this
406 process, alone or in concert with upregulation of γδ T cells as well as increases in circulating IL-
407 10, may contribute to systemic hypo-inflammation in some patients. Given the difficulty in
408 teasing apart these processes (especially given the need to assess IL-22 in tissues of human
409 trauma patients), this hypothesis may require studies in animal models or advances in the ability
410 to detect fluxes in cell populations in humans *in situ* (61).
411 Another intriguing hypothesis that will need to be tested further is that of the apparent
412 "phase shift" in an oscillatory systemic inflammatory response inferred via DyNA when
413 stratifying trauma patients based on homozygous genotype at rs4774381. In unpublished studies,
414 we have inferred similar dynamic network oscillations when examining the systemic
415 inflammatory responses of spinal cord injury patients segregated based on the location of their
416 spinal cord injury (T6 and above vs. below T6; R. Zamora, E. Robbins, W. Huang, Y. Vodovotz,
417 and G. Sowa, unpublished), which raises the possibility of neural involvement in this
418 phenomenon. In support of this hypothesis, we have previously documented a role for the
419 chemokine IP-10/CXCL10 as a driver of IL-10 and systemic hypo-inflammation when
420 comparing trauma patients with vs. without spinal cord injury (62).
421 rs11919443 in the *TM4SF19* gene was another key SNP inferred to be related to
422 dysregulated systemic inflammation (including distinct IL-17A time courses as a function of
423 genotype at this SNP). Specifically, patients with the homozygous AA genotype of rs11919443
424 exhibited significantly longer ICU length of stay and requirement for mechanical ventilation
425 (along with a trend towards longer total hospital length of stay) as well as higher circulating IL-
426 17A levels as compared to patients with the alternative homozygous (BB) genotype.
427 Transmembrane 4 L six family member 19 (TM4SF19) is a lysosomal protein that suppresses
428 acidification; its inactivation was found to block the increase in accumulation of macrophages in
429 a murine adipose tissue and thus was associated with reduced inflammation (63). *In vitro* studies
430 suggested that TM4SF19 exacerbates the effects of bacterial lipopolysaccharide on human
431 venous endothelial cells by impacting the expression of cell junction proteins (64). Thus,
432 TM4SF19 appears to exert pro-inflammatory effects, albeit indirectly.
433 One such indirect mechanism appears to involve the chemokine CXCL2, based on a
434 recent bioinformatics study linking TM4SF19 and CXCL2 in the context of childhood obesity
435 (65). Interleukin-17A induced CXCL2 among its many actions (66), and bioinformatics analyses
436 have therefore placed CXCL2 in the IL-17A signaling pathway (67, 68). Furthermore, IL-17A

437 synergizes with TNF-α to drive endothelial expression of CXCL2 and subsequent neutrophil
438 recruitment (69).
439 A key aspect of the present study is the focus on a control group of SNPs selected based
440 on the following criteria: 1) absence of statistically significant differences in circulating
441 inflammatory mediators between subgroups of trauma patients stratified on the basis of their
442 homozygous genotype at a given SNP, and 2) presence of statistically significant differences in
443 clinical outcomes in these same patients. Once SNPs that met these criteria were selected,
444 FLAME analysis was used to define hub genes. This analysis identified *SLC2A1* as the main hub
445 gene. SLC2A1 (solute carrier family 2, facilitated glucose transporter member 1/glucose
446 transporter 1 [GLUT1]) is the main glucose transporter (70), in which there has been extensive
447 interest due to the emerging role of glucose metabolism in autoimmunity (71, 72), cancer (73,
448 74), as well as sepsis-induced critical illness (75). Our findings support a role for differential
449 glucose transport in organ dysfunction in the context of trauma-induced critical illness as well.
450 Our study has several limitations. These include the need to assess more SNPs and other
451 genetic variants in larger, more diverse patient cohorts; to measure more mediators to better
452 define the impact of the specific SNPs assessed herein on the immuno-inflammatory response;
453 and to assess other 'omics layers to better delineate the host's pathophysiological response in the
454 context of genetic predisposition. Computational modeling – adding mechanistic modeling to
455 the present study's data-driven modeling approaches (61) – would also serve an important role in
456 any attempt to connect our findings to the host's pathophysiology following severe traumatic
457 injury and would also help address the network of interaction among SNPs (76, 77). Finally, our
458 conclusions are based on associations rather than direct mechanistic work, though our initial
459 study documenting the role of IL-17A in the injury response included supportive mechanistic
460 studies involving neutralization of IL-17A in a mouse model of trauma/hemorrhage (13).
461 Despite these limitations, the present study suggests a clear role for nuanced Th17
462 response in the context of trauma-associated systemic inflammation and critical illness. Multiple
463 cell types can express IL-17A, including Th17 cells, δγ T cells, and innate lymphoid cells (ILCs)
464 (44-50). In the context of trauma-associated critical illness or experimental models of
465 trauma/hemorrhage, IL-17A production is associated with morbidity and mortality (13, 15, 19-
466 21). While studies have implicated both Th17 cells (13, 40) and ILCs (78) in this
467 pathophysiology, the present study points to RORA and Th17 differentiation as a key genetically
468 regulated aspect of this response; future studies will hopefully address the relative contributions
469 of these distinct cell populations.

470 **REFERENCES**

471 1. Horiguchi H, Loftus TJ, Hawkins RB, Raymond SL, Stortz JA, Hollen MK, et al. Innate
472 immunity in the Persistent nflammation, mmunosuppression, and Catabolism Syndrome and its
473 implications for therapy. Frontiers in immunology. 2018;9:595.
474 2. Lord JM, Midwinter MJ, Chen YF, Belli A, Brohi K, Kovacs EJ, et al. The systemic
475 immune response to trauma: an overview of pathophysiology and treatment. Lancet.
476 2014;384(9952):1455-65.
477 3. Huber-Lang M, Lambris JD, Ward PA. Innate immune responses to trauma. Nature
478 immunology. 2018;19(4):327-41.
479 4. Lamparello AJ, Namas RA, Constantine G, McKinley TO, Elster E, Vodovotz Y, et al. A
480 conceptual time window-based model for the early stratification of trauma patients. Journal of
481 internal medicine. 2019.
482 5. Hildebrand F, Mommsen P, Frink M, van Griensven M, Krettek C. Genetic
483 predisposition for development of complications in multiple trauma patients. Shock (Augusta,
484 Ga). 2011;35(5):440-8.
485 6. Lamparello AJ, Namas RA, Abdul-Malak O, Vodovotz Y, Billiar TR. Young and aged
486 blunt trauma patients display major differences in circulating inflammatory mediator profiles
487 after severe injury. Journal of the American College of Surgeons. 2019;228:148-60.e7.
488 7. Zaaqoq AM, Namas RA, Abdul-Malak O, Almahmoud K, Barclay D, Yin J, et al.
489 Diurnal variation in systemic acute inflammation and clinical outcomes following severe blunt
490 trauma. Frontiers in immunology. 2019;10(2699).
491 8. Almahmoud K, Namas RA, Zaaqoq AM, Abdul-Malak O, Namas R, Zamora R, et al.
492 Prehospital hypotension is associated with altered inflammation dynamics and worse outcomes
493 following blunt trauma in humans. Critical care medicine. 2015;43:1395-404.
494 9. Almahmoud K, Namas RA, Abdul-Malak O, Zaaqoq AM, Zamora R, Zuckerbraun BS, et
495 al. Impact of injury severity on dynamic inflammation networks following blunt trauma. Shock
496 (Augusta, Ga). 2015;44:105-9.
497 10. Abdul-Malak O, Vodovotz Y, Zaaqoq A, Guardado J, Almahmoud K, Yin J, et al.
498 Elevated admission base deficit is associated with a complex dynamic network of systemic
499 inflammation which drives clinical trajectories in blunt trauma patients. Mediators of
500 inflammation. 2016;2016:7950374. http://dx.doi.org/10.1155/2016/.
501 11. Almahmoud K, Abboud A, Namas RA, Zamora R, Sperry J, Peitzman AB, et al.
502 Computational evidence for an early, amplified systemic inflammation program in polytrauma
503 patients with severe extremity injuries. PloS one. 2019;14(6):e0217577.
504 12. Namas RA, Vodovotz Y, Almahmoud K, Abdul-Malak O, Zaaqoq A, Namas R, et al.
505 Temporal patterns of circulating inflammation biomarker networks differentiate susceptibility to
506 nosocomial infection following blunt trauma in humans. Ann Surg. 2016;263:191-8.
507 13. Abboud AN, Namas RA, Ramadan M, Mi Q, Almahmoud K, Abdul-Malak O, et al.
508 Computational analysis supports an early, type 17 cell-associated divergence of blunt trauma
509 survival and mortality. Crit Care Med. 2016;44:e1074-e81.
510 14. Namas R, Almahmoud K, Mi Q, Ghuma A, Namas R, Zaaqoq A, et al. Individual-
511 specific principal component analysis of circulating inflammatory mediators predicts early organ
512 dysfunction in trauma patients. Journal of critical care. 2016;36:146-53.

513 15. Schimunek L, Lindberg H, Cohen M, Namas RA, Mi Q, Yin J, et al. Computational
514 derivation of core, dynamic human blunt trauma inflammatory endotypes. Frontiers in
515 immunology. 2021;11(3481).
516 16. Liu D, Namas RA, Vodovotz Y, Peitzman AB, Simmons RL, Yuan H, et al.
517 Unsupervised clustering analysis based on MODS severity identifies four distinct organ
518 dysfunction patterns in severely injured blunt trauma patients. Frontiers in medicine. 2020;7(46).
519 17. Wu J, Vodovotz Y, Abdelhamid S, Guyette FX, Yaffe MB, Gruen DS, et al. Multi-omic
520 analysis in injured humans: Patterns align with outcomes and treatment responses. Cell Reports
521 Medicine. 2021;2(12).
522 18. Wu J, Cyr A, Gruen DS, Lovelace TC, Benos PV, Das J, et al. Lipidomic signatures align
523 with inflammatory patterns and outcomes in critical illness. Nature communications. 2022;13(1).
524 19. Schimunek L, Namas RA, Yin J, Liu D, Barclay D, El-Dehaibi F, et al. An enrichment
525 strategy yields seven novel single nucleotide polymorphisms associated with mortality and
526 altered TH17 responses following blunt trauma. Shock (Augusta, Ga). 2018;49:259-68.
527 20. Zamora R, Forsberg JA, Shah AM, Unselt D, Grey S, Lisboa FA, et al. Central role for
528 neurally dysregulated IL-17A in dynamic networks of systemic and local inflammation in
529 combat casualties. Scientific reports. 2023;13(1).
530 21. Shah AM, Zamora R, Vodovotz Y. Interleukin-17 as a spatiotemporal bridge from acute
531 to chronic inflammation: Novel insights from computational modeling. WIREs Mechanisms of
532 Disease. 2023;e1599.
533 22. Schimunek L, Namas RA, Yin J, Barclay D, Liu D, el-Dehaibi F, et al. MPPED2
534 polymorphism is associated with altered systemic inflammation and adverse trauma outcomes.
535 Frontiers in genetics. 2019;10(1115).
536 23. Lamparello AJ, Namas RA, Schimunek L, Cohen M, El-Dehaibi F, Yin J, et al. An
537 aging-related single-nucleotide polymorphism is associated with altered clinical outcomes and
538 distinct inflammatory profiles in aged blunt trauma patients. Shock (Augusta, Ga). 2020;53:146-
539 55.
540 24. El-Dehaibi F, Zamora R, Radder J, Yin J, Shah AM, Namas RA, et al. A common single
541 nucleotide polymorphism is associated with inflammation and critical illness outcomes. iScience.
542 2023;26(12):108333.
543 25. El-Dehaibi F, Zamora R, Yin J, Namas RA, Billiar TR, Vodovotz Y. Network analysis of
544 single-nucleotide polymorphisms associated with aberrant inflammation in trauma patients
545 suggests a role for vesicle-associated inflammatory programs involving CD55. Shock (Augusta,
546 Ga). 2024:10.1097/SHK.0000000000002448.
547 26. BAKER SP, O'NEILL B, HADDON WJ, LONG WB. The injury severity score: A
548 method for describing patients with multiple injuries and evaluating emergency care. Journal of
549 Trauma and Acute Care Surgery. 1974;14(3):187-96.
550 27. Gennarelli TA, Wodzin E. AIS 2005: a contemporary injury scale. Injury.
551 2006;37(12):1083-91.
552 28. Marshall JC, Cook DJ, Christou NV, Bernard GR, Sprung CL, Sibbald WJ. Multiple
553 organ dysfunction score: a reliable descriptor of a complex clinical outcome. Critical care
554 medicine. 1995;23(10):1638-52.

555 29. Karatzas E, Baltoumas FA, Aplakidou E, Kontou PI, Stathopoulos P, Stefanis L, et al.
556 Flame (v2.0): advanced integration and interpretation of functional enrichment results from
557 multiple sources. Bioinformatics. 2023;39(8).
558 30. Kolberg L, Raudvere U, Kuzmin I, Adler P, Vilo J, Peterson H. g:Profiler-interoperable
559 web service for functional enrichment analysis and gene identifier mapping (2023 update).
560 Nucleic Acids Res. 2023;51(W1):W207-W12.
561 31. Xie Z, Bailey A, Kuleshov MV, Clarke DJB, Evangelista JE, Jenkins SL, et al. Gene Set
562 Knowledge Discovery with Enrichr. Curr Protoc. 2021;1(3):e90.
563 32. Aleksander S, Balhoff J, Carbon S, Cherry J, Drabkin H, Ebert D, et al. The Gene
564 Ontology knowledgebase in 2023., 2023, 224, p. iyad031. DOI: https://doi
565 org/101093/genetics/iyad031 PMID: https://www ncbi nlm nih gov/pubmed/36866529.
566 33. Kanehisa M, Goto S. KEGG: kyoto encyclopedia of genes and genomes. Nucleic Acids
567 Res. 2000;28(1):27-30.
568 34. Ziraldo C, Vodovotz Y, Namas RA, Almahmoud K, Tapias V, Mi Q, et al. Central role
569 for MCP-1/CCL2 in injury-induced inflammation revealed by in vitro, in silico, and clinical
570 studies. PLoS One. 2013;8(12):e79804.
571 35. Abboud A, Namas RA, Ramadan M, Mi Q, Almahmoud K, Abdul-Malak O, et al.
572 Computational Analysis Supports an Early, Type 17 Cell-Associated Divergence of Blunt
573 Trauma Survival and Mortality. Crit Care Med. 2016;44(11):e1074-e81.
574 36. Zamora R, Korff S, Mi Q, Barclay D, Schimunek L, Zucca R, et al. A computational
575 analysis of dynamic, multi-organ inflammatory crosstalk induced by endotoxin in mice. PLoS
576 Comput Biol. 2018;14(11):e1006582.
577 37. Auton A, Abecasis GR, Altshuler DM, Durbin RM, Abecasis GR, Bentley DR, et al. A
578 global reference for human genetic variation. Nature. 2015;526(7571):68-74.
579 38. Korn T, Bettelli E, Oukka M, Kuchroo VK. IL-17 and Th17 Cells. Annu Rev Immunol.
580 2009;27:485-517.
581 39. Mi Q, Constantine G, Ziraldo C, Solovyev A, Torres A, Namas R, et al. A dynamic view
582 of trauma/hemorrhage-induced inflammation in mice: Principal drivers and networks. PloS one.
583 2011;6:e19424.
584 40. Seshadri A, Brat GA, Yorkgitis BK, Keegan J, Dolan J, Salim A, et al. Phenotyping the
585 immune response to trauma: A multiparametric systems immunology approach. Critical care
586 medicine. 2017;45:1523-30.
587 41. Kovrigina E, Wesolowski D, Altman S. Coordinate inhibition of expression of several
588 genes for protein subunits of human nuclear RNase P. Proceedings of the National Academy of
589 Sciences of the United States of America. 2003;100(4):1598-602.
590 42. Brown D, Namas RA, Almahmoud K, Zaaqoq A, Sarkar J, Barclay DA, et al. Trauma *in*
591 *silico*: individual-specific mathematical models and virtual clinical populations. Science
592 translational medicine. 2015;7:285ra61.
593 43. Sperry JLZ, S.; Zuckerbraun, B.S.; Vodovotz, Y.; Namas, R.; Ferrell, R.E.; Rosengart,
594 M.R.; Peitzman, A.B.; Billiar, T.R. . X-chromosome linked IRAK1 polymorphism is a strong
595 predictor of multiple organ failure and mortality post-injury. Ann Surg. 2014;260:698-703.
596 44. Lillehoj HS, Lillehoj EP, Weinstock D, Schat KA. Functional and biochemical
597 characterizations of avian T lymphocyte antigens identified by monoclonal antibodies. European
598 Journal of Immunology. 1988;18(12):2059-65.

599 45. Park H, Li Z, Yang XO, Chang SH, Nurieva R, Wang Y-H, et al. A distinct lineage of
600 CD4 T cells regulates tissue inflammation by producing interleukin 17. Nature Immunology.
601 2005;6(11):1133-41.
602 46. Chan MM, Chen CL, Ager LL, Cooper MD. Identification of the avian homologues of
603 mammalian CD4 and CD8 antigens. J Immunol. 1988;140(7):2133-8.
604 47. Harrington LE, Hatton RD, Mangan PR, Turner H, Murphy TL, Murphy KM, et al.
605 Interleukin 17–producing CD4+ effector T cells develop via a lineage distinct from the T helper
606 type 1 and 2 lineages. Nature Immunology. 2005;6(11):1123-32.
607 48. McGeachy MJ, Cua DJ, Gaffen SL. The IL-17 Family of Cytokines in Health and
608 Disease. Immunity. 2019;50(4):892-906.
609 49. Skopelja-Gardner S, Tai J, Sun X, Tanaka L, Kuchenbecker JA, Snyder JM, et al. Acute
610 skin exposure to ultraviolet light triggers neutrophil-mediated kidney inflammation. Proc Natl
611 Acad Sci U S A. 2021;118(3).
612 50. Cua DJ, Tato CM. Innate IL-17-producing cells: the sentinels of the immune system. Nat
613 Rev Immunol. 2010;10(7):479-89.
614 51. Beringer A, Noack M, Miossec P. IL-17 in Chronic Inflammation: From Discovery to
615 Targeting. Trends in Molecular Medicine. 2016;22(3):230-41.
616 52. Flierl MA, Rittirsch D, Gao H, Hoesel LM, Nadeau BA, Day DE, et al. Adverse
617 functions of IL-17A in experimental sepsis. Faseb j. 2008;22(7):2198-205.
618 53. Bosmann M, Ward PA. Therapeutic potential of targeting IL-17 and IL-23 in sepsis. Clin
619 Transl Med. 2012;1(1):4.
620 54. Xu Z, Shi L, Wang Y, Zhang J, Huang L, Zhang C, et al. Pathological findings of
621 COVID-19 associated with acute respiratory distress syndrome. Lancet Respir Med.
622 2020;8(4):420-2.
623 55. Konieczny P, Xing Y, Sidhu I, Subudhi I, Mansfield KP, Hsieh B, et al. Interleukin-17
624 governs hypoxic adaptation of injured epithelium. Science. 2022;377(6602):eabg9302.
625 56. Shah AM, Aral AM, Zamora R, Gharpure N, El-Dehaibi F, Zor F, et al. Peripheral nerve
626 repair is associated with augmented cross-tissue inflammation following vascularized composite
627 allotransplantation. Frontiers in immunology. 2023;14.
628 57. Bettelli E, Carrier Y, Gao W, Korn T, Strom TB, Oukka M, et al. Reciprocal
629 developmental pathways for the generation of pathogenic effector TH17 and regulatory T cells.
630 Nature. 2006;441(7090):235-8.
631 58. Lee Y, Awasthi A, Yosef N, Quintana FJ, Xiao S, Peters A, et al. Induction and
632 molecular signature of pathogenic TH17 cells. Nature immunology. 2012;13(10):991-9.
633 59. Ouyang W, O'Garra A. IL-10 family cytokines IL-10 and IL-22: from basic science to
634 clinical translation. Immunity. 2019;50(4):871-91.
635 60. Cai J, McKinley T, Billiar I, Zenati MS, Gaski G, Vodovotz Y, et al.
636 Protective/reparative cytokines are suppressed at high injury severity in human trauma. Trauma
637 surgery & acute care open. 2021;6(1):e000619.
638 61. Vodovotz Y. Towards systems immunology of critical illness at scale: from single cell
639 'omics to digital twins. Trends Immunol. 2023;44:345-55.
640 62. Zaaqoq AM, Namas R, Almahmoud K, Azhar N, Mi Q, Zamora R, et al. Inducible
641 protein-10, a potential driver of neurally-controlled IL-10 and morbidity in human blunt trauma.
642 CritCare Med. 2014;42:1487-97.

643 63. Choi C, Jeong YL, Park KM, Kim M, Kim S, Jo H, et al. TM4SF19-mediated control of
644 lysosomal activity in macrophages contributes to obesity-induced inflammation and metabolic
645 dysfunction. Nature communications. 2024;15(1):2779.
646 64. Ding L, Li LM, Hu B, Wang JL, Lu YB, Zhang RY, et al. TM4SF19 aggravates LPS-
647 induced attenuation of vascular endothelial cell adherens junctions by suppressing VE-cadherin
648 expression. Biochemical and biophysical research communications. 2020;533(4):1204-11.
649 65. He E, Chang K, Dong L, Jia M, Sun W, Cui H. Identification and validation of CXCL2
650 as a key gene for childhood obesity. Biochem Genet. 2024;62(4):2743-65.
651 66. Onishi RM, Gaffen SL. Interleukin-17 and its target genes: mechanisms of interleukin-17
652 function in disease. Immunology. 2010;129(3):311-21.
653 67. Cao M, Wang Y. Bioinformatic analyses determine the importance of CXCL2 and
654 CXCL8 in atypical meningioma development and reoccurrence. Turk Neurosurg.
655 2022;32(3):430-41.
656 68. Sun Y, Cai D, Hu W, Fang T. Identifying hub genes and miRNAs in Crohn's disease by
657 bioinformatics analysis. Frontiers in genetics. 2022;13:950136.
658 69. Griffin GK, Newton G, Tarrio ML, Bu DX, Maganto-Garcia E, Azcutia V, et al. IL-17
659 and TNF-α sustain neutrophil recruitment during inflammation through synergistic effects on
660 endothelial activation. Journal of immunology (Baltimore, Md : 1950). 2012;188(12):6287-99.
661 70. Brown GK. Glucose transporters: structure, function and consequences of deficiency. J
662 Inherit Metab Dis. 2000;23(3):237-46.
663 71. Palmer CS, Hussain T, Duette G, Weller TJ, Ostrowski M, Sada-Ovalle I, et al.
664 Regulators of glucose metabolism in CD4(+) and CD8(+) T cells. Int Rev Immunol.
665 2016;35(6):477-88.
666 72. Di Dedda C, Vignali D, Piemonti L, Monti P. Pharmacological targeting of GLUT1 to
667 control autoreactive T cell responses. International journal of molecular sciences. 2019;20(19).
668 73. Gonzalez-Menendez P, Hevia D, Mayo JC, Sainz RM. The dark side of glucose
669 transporters in prostate cancer: Are they a new feature to characterize carcinomas? Int J Cancer.
670 2018;142(12):2414-24.
671 74. Alves AP, Mamede AC, Alves MG, Oliveira PF, Rocha SM, Botelho MF, et al.
672 Glycolysis inhibition as a strategy for hepatocellular carcinoma treatment? Curr Cancer Drug
673 Targets. 2019;19(1):26-40.
674 75. Deane AM, Rayner CK, Keeshan A, Cvijanovic N, Marino Z, Nguyen NQ, et al. The
675 effects of critical illness on intestinal glucose sensing, transporters, and absorption. Critical care
676 medicine. 2014;42(1):57-65.
677 76. Pairo-Castineira E, Rawlik K, Bretherick AD, Qi T, Wu Y, Nassiri I, et al. GWAS and
678 meta-analysis identifies 49 genetic variants underlying critical COVID-19. Nature.
679 2023;617(7962):764-8.
680 77. Yang D, Jin Y, He X, Dong A, Wang J, Wu R. Inferring multilayer interactome networks
681 shaping phenotypic plasticity and evolution. Nature communications. 2021;12(1):5304.
682 78. Manson J, Hoffman R, Chen S, Ramadan MH, Billiar TR. Innate-like lymphocytes are
683 immediate participants in the hyper-acute immune response to trauma and hemorrhagic shock.
684 Frontiers in immunology. 2019;10:1501.

685 79. El-Dehaibi F, Zamora R, Yin J, Billiar TR, Vodovotz Y. medRxiv. 2025.01.28.25321184
686 [Preprint]. Available at https://www.medrxiv.org/content/10.1101/2025.01.28.25321184v2
687 (Accessed June 13, 2025).

688 **ABBREVIATIONS**
689
690 ABI3BP: ABI family member 3 binding protein
691 AIS: Abbreviated Injury Scale
692 ANOVA: Analysis of Variance
693 DyNA: Dynamic Network Analysis
694 GLUT1: glucose transporter 1
695 GM-CSF: granulocyte-macrophage colony stimulating factor
696 GO: Gene Ontology Knowledgebase
697 ICU: intensive care unit
698 IFN: interferon
699 IL: Interleukin
700 ILC: innate lymphoid cell
701 IP-10: IFN-γ inducible protein (CXCL10)
702 IL: interleukin
703 IQSEC2: IQ motif and Sec7 domain ArfGEF 2
704 ISS: Injury Severity Score
705 KEGG: Kyoto Encyclopedia of Genes and Genomics
706 LOS: length of stay
707 LYPD4: LY6/PLAUR domain containing 4
708 MCP: monocyte chemotactic protein
709 MIG: monokine induced by gamma interferon (CXCL9)
710 MIP: macrophage inflammatory protein
711 MODS: Multiple Organ Dysfunction Syndrome
712 NMT2: N-myristoyltransferase 2
713 RGS21: regulator of G protein signaling 21
714 RPP38: ribonuclease P/MRP subunit p38
715 RORA: RAR-related orphan receptor A
716 SLC2A1: solute carrier family 2, facilitated glucose transporter member 1
717 SNP: single nucleotide polymorphism
718 sST2: soluble suppression of tumorigenicity-2
719 TM4SF19: transmembrane 4 L six family member 19
720 TNF-α: tumor necrosis factor α
721 UBE2D2: ubiquitin conjugating enzyme E2 D2

FUNDING

This work was supported by Department of Defense grant W81XWH-18-2-0051 and Defense Advanced Research Projects Agency grant D20AC00002.

ACKNOWLEDGMENTS

This work was made possible by the Department of Defense and the Defense Advanced Research Projects Agency. The manuscript was first published as a preprint to medRxiv.org.

AUTHOR CONTRIBUTIONS

FE: Writing, software development, data analysis, investigation, visualization. RZ: Writing, data analysis, visualization. JY: Inflammatory mediator arrays, genomic analysis. TB: Curation of patient data, review and editing. YZ: Conceptualization, writing, review and editing, project administration, funding acquisition. This manuscript has been read and approved by all authors.

CONFLICT OF INTEREST

The authors declare that the research was conducted in the absence of any commercial or financial relationships that could be construed as a potential conflict of interest.

739 **FIGURE CAPTIONS**
740 **Figure 1. FLAME tree plot describing molecular function connectivity of 'rare' SNPs**
741 **implicated in inflammatory biomolecules disparity by *SNPScanner*.** These results were found
742 in the Gene Ontology knowledgebase with the web tool *enrichR*. SNP rs4774381 corresponds to
743 the gene for RORA, which is a component of the mTORc1 complex in a Th17 differentiation
744 pathway.
745
746 **Figure 2. Distinct trajectories of circulating inflammatory mediator mediators as a function**
747 **of homozygous genotype at rs4774381. (A)** Statistically distinct (*$p < 0.05$ by Two-Way
748 ANOVA) circulating inflammatory biomarker concentrations from 4 hours to 7 days past
749 admission between patients with rs4774381^{AA} and rs4774381^{BB}. **(B)** Marshall MODS seven-day
750 time course between rs4774381^{AA} and rs4774381^{BB} patients (*$p < 0.001$ by Two-Way ANOVA).
751
752 **Figure 3. Dynamic network analysis (DyNA) suggests distinct inflammatory programs as a**
753 **function of homozygous genotype at rs4774381.** DyNA results for inflammatory biomolecules
754 from 4h-D7 of rs4774381^{AA} patients **(A)** and rs4774381^{BB} patients **(B)**. A representative DyNA
755 output showing all inflammatory mediators in the networks is also shown to easily identify the
756 mediators. **(C)** Graph of dynamic network complexity over the 4h-D7 time course between
757 rs4774381^{AA} and rs4774381^{BB}. **(D)** Table of the total number of connections for each
758 biomolecule for both rs4774381 genotypes.
759
760 **Figure 4.** Spearman's correlations of IL-17A and Th17 differentiation-associated biomolecules:
761 GM-CSF **(A** and **E)**, IL-10 **(B** and **F)**, TNF-α **(C** and **G)** and IL-22 **(D** and **H)**. Panels **(A-D)** are
762 correlations performed for rs4774381^{AA} and panels **(E-H)** are those for rs4774381^{BB}.
763
764 **Figure 5. Distinct IL-17A trajectories and clinical outcomes as a function of homozygous**
765 **genotype at rs11919443. (A-C)** Post-admission comparison of systemic inflammation and
766 clinical outcomes between rs11919443^{AA} and rs11919443^{BB}. **(A)** rs11919443^{AA} patients
767 exhibited a significant spike in IL-17A concentration from 20 hours to 2 days post-injury
768 compared to rs11919443^{BB} patients. **(B-C)** Patients with rs11919443^{AA} had significantly longer
769 ICU stays and required more days on mechanical ventilation than rs11919443^{BB}.
770
771 **Figure 6. Dynamic network analysis suggests distinct inflammatory programs and the**
772 **presence of hypo-inflammation as a function of homozygous genotype at rs11919443. (A)**
773 Graph of dynamic network complexity over the 4h-D7 time course between rs11919443 ^{AA} and
774 rs11919443 ^{BB}. **(B)** Table of the total number of connections for each biomolecule for both
775 rs11919443 genotypes.
776
777 **Figure 7. Correlation-based inference of Th17 cell subsets as a function of homozygous**
778 **genotype at rs11919443.** Spearman's correlations for rs11919443^{AA} **(A-D)** and rs11919443^{BB}
779 **(E-H)** of IL-17A and Th17 differentiation-associated biomolecules: GM-CSF **(A** and **E)**, IL-10
780 **(B** and **F)**, TNF-α **(C** and **G)**, and IL-22 **(D** and **H)**.
781

782 **Figure 8. (A-B) FLAME tree plot describing molecular function connectivity of 'rare' SNPs**
783 **with no significant inflammatory biomarker disparity, according to *SNPScanner*.** These
784 results were found in the Gene Ontology knowledgebase with the web tools *gProfiler* **(A)** and
785 *enrichR* **(B)**. Clinical parameter analysis by two-way ANOVA failed to reveal differences in ISS
786 **(C)** and AIS **(D)** between $rs841852^{AA}$ and $rs841852^{BB}$, but implicated significant differences ($p <$
787 0.05) for days in the ICU **(E)**, total hospital days **(F)**, and Marshall MODS **(G)**.
788
789 **Figure 9. Distinct trajectories of circulating inflammatory mediator mediators as a function**
790 **of homozygous genotype at rs841852**. Statistically significantly different ($p < 0.05$ by two-way
791 ANOVA) biomarkers: IL-1RA **(A)**, IL-7 **(B)**, IL-13 **(C)**, IL-15 **(D)**, MIG **(E)**, and sIL-2Ra **(F)**.
792
793 **Figure 10. Dynamic network analysis suggests distinct inflammatory programs and the**
794 **presence of hypo-inflammation as a function of homozygous genotype at rs841852. (A)**
795 Network complexity of inflammatory biomolecules from 4h-D7 for rs841852 homozygous
796 genotypes. **(B)** Table of total network connections for all inflammatory biomolecules for both
797 genotypes.
798
799 **Figure 11.** Spearman's correlations for $rs841852^{AA}$ **(A-D)** and $rs841852^{BB}$ **(E-H)** of IL-17A and
800 Th17 differentiation-associated biomolecules: GM-CSF **(A** and **E)**, IL-10 **(B** and **F)**, TNF-α **(C**
801 and **G)**, and IL-22 **(D** and **H)**.

Figure 1

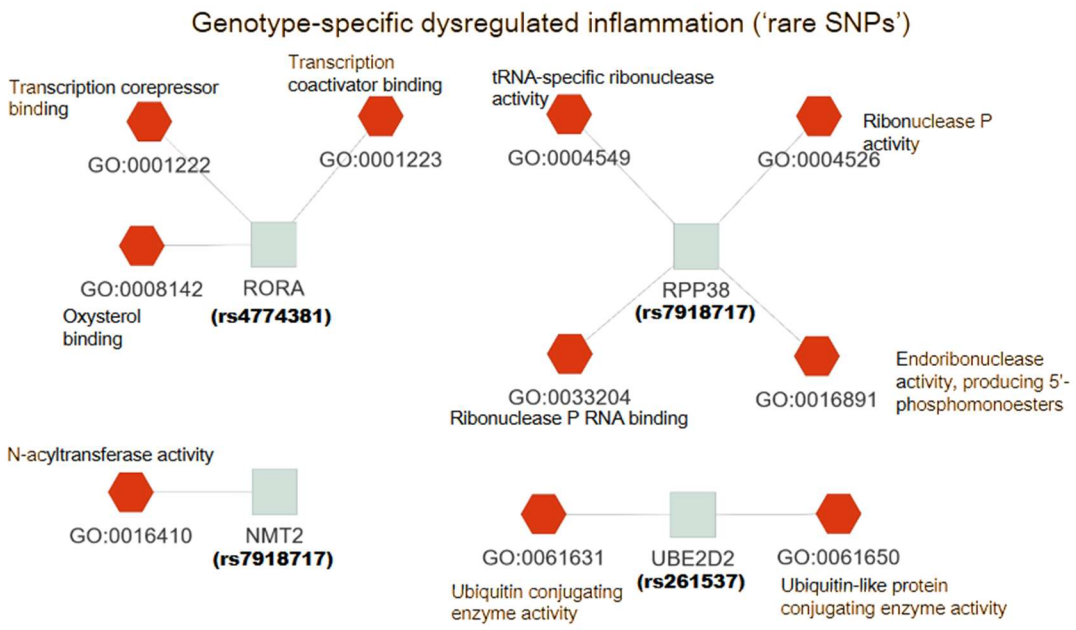

802
803

Figure 2

A

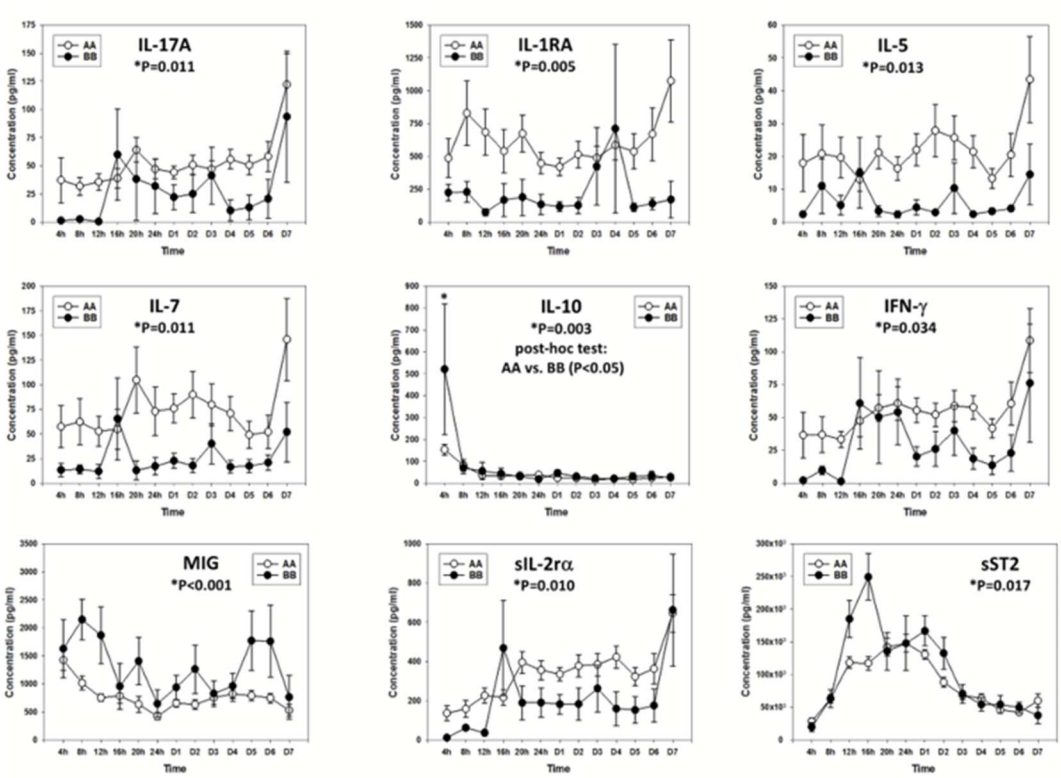
IL-17A
*P=0.011
IL-1RA
*P=0.005
IL-5
*P=0.013
IL-7
*P=0.011
IL-10
*P=0.003
post-hoc test:
AA vs. BB (P<0.05)
IFN-γ
*P=0.034
MIG
*P<0.001
sIL-2rα
*P=0.010
sST2
*P=0.017
AA
BB
Concentration (pg/ml)
Time
4h 8h 12h 16h 20h 24h D1 D2 D3 D4 D5 D6 D7

806

Figure 2

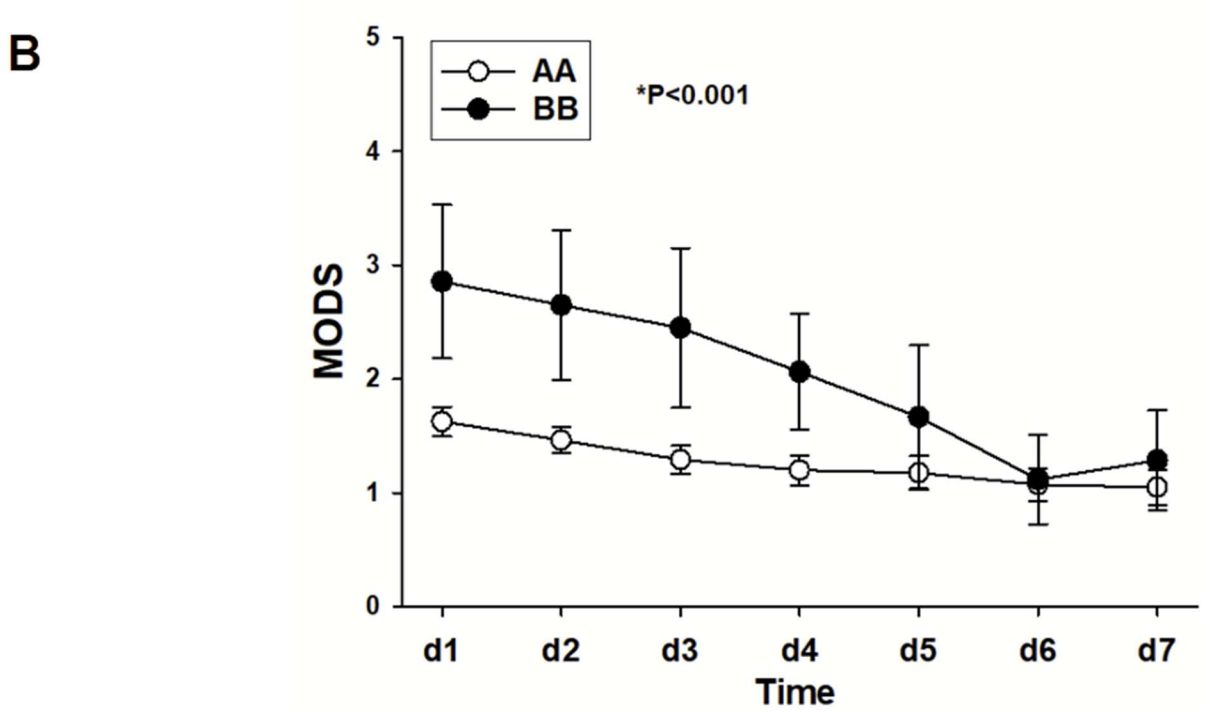

807
808

Figure 3

A

AA

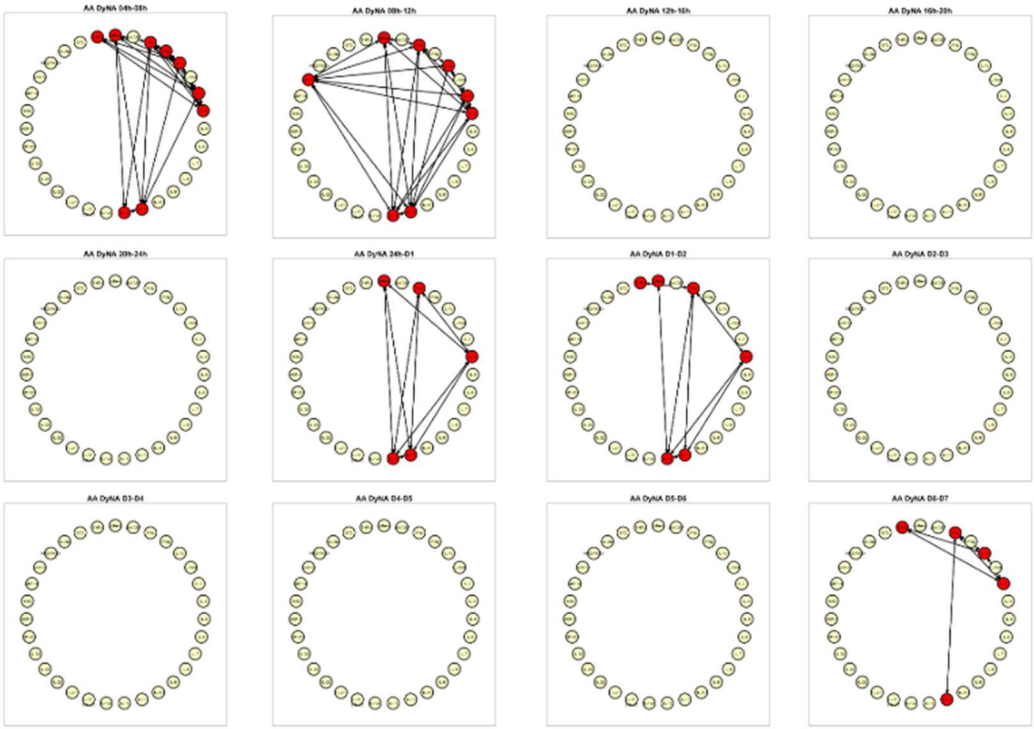
AA DyNA 04h-08h
AA DyNA 08h-12h
AA DyNA 12h-16h
AA DyNA 16h-20h
AA DyNA 20h-24h
AA DyNA 24h-D1
AA DyNA D1-D2
AA DyNA D2-D3
AA DyNA D3-D4
AA DyNA D4-D5
AA DyNA D5-D6
AA DyNA D6-D7

Figure 3

B

BB

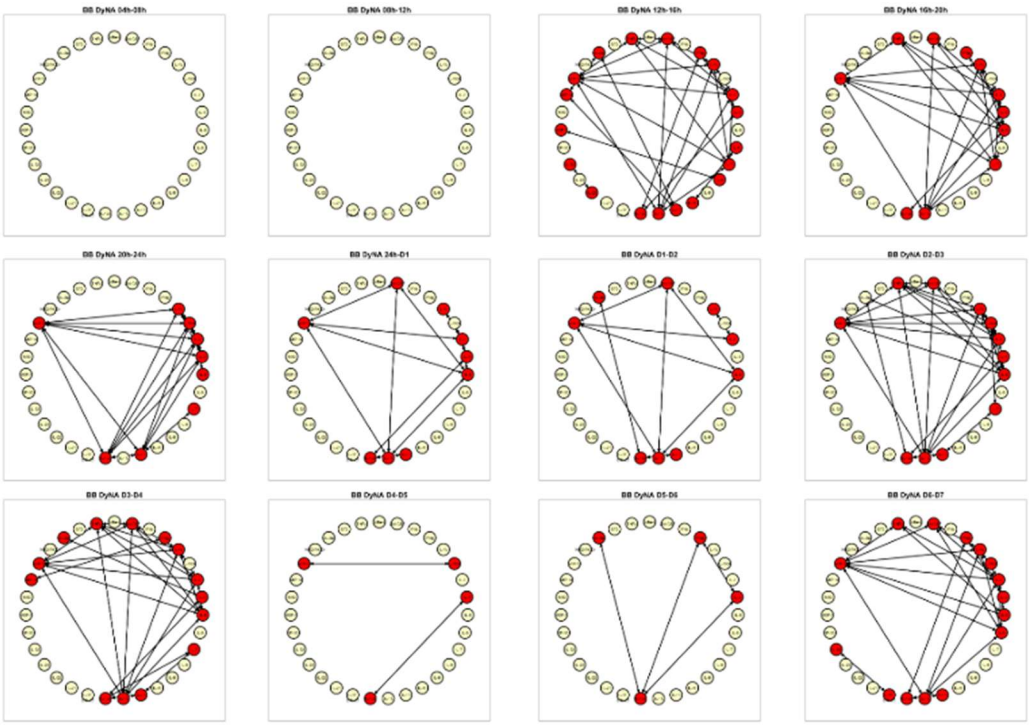

811
812

Figure 3

C

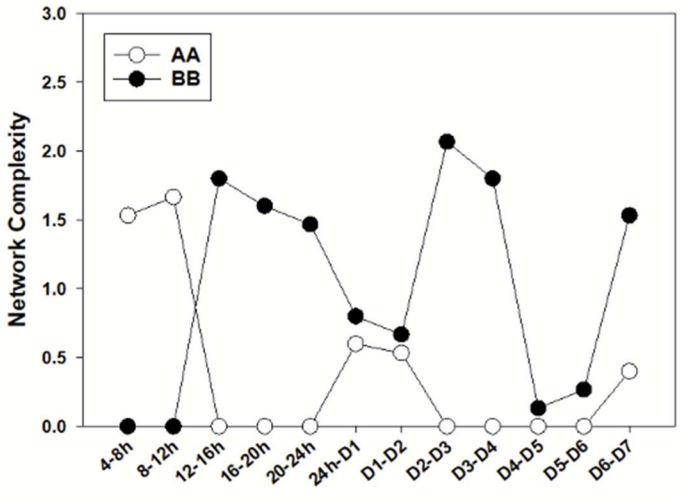

D

Total Connectivity	AA 0.95	BB 0.95
MIP-1b	7	47
IL-2	16	45
IL-1b	15	34
IL-15	17	33
IL-5	0	31
GM-CSF	0	29
IL-17A	0	25
TNFa	6	24
IL-4	19	20
IL-7	0	16
IL-13	20	15
IL-1RA	0	14
IFNg	4	8
sIL-2ra	0	7
IL-6	0	6
MIP-1a	0	3
IL-33	0	2
Eotaxin	14	0
IFNa	24	0
IL-8	0	1
IL-10	0	1
IL-17E/IL-25	0	1
IL-22	0	1
MCP-1	0	1
IL-9	0	0
IL-21	0	0
IL-23	0	0
IP-10	0	0
MIG	0	0
NO2-/NO3-	0	0
ST2	0	0

Figure 4

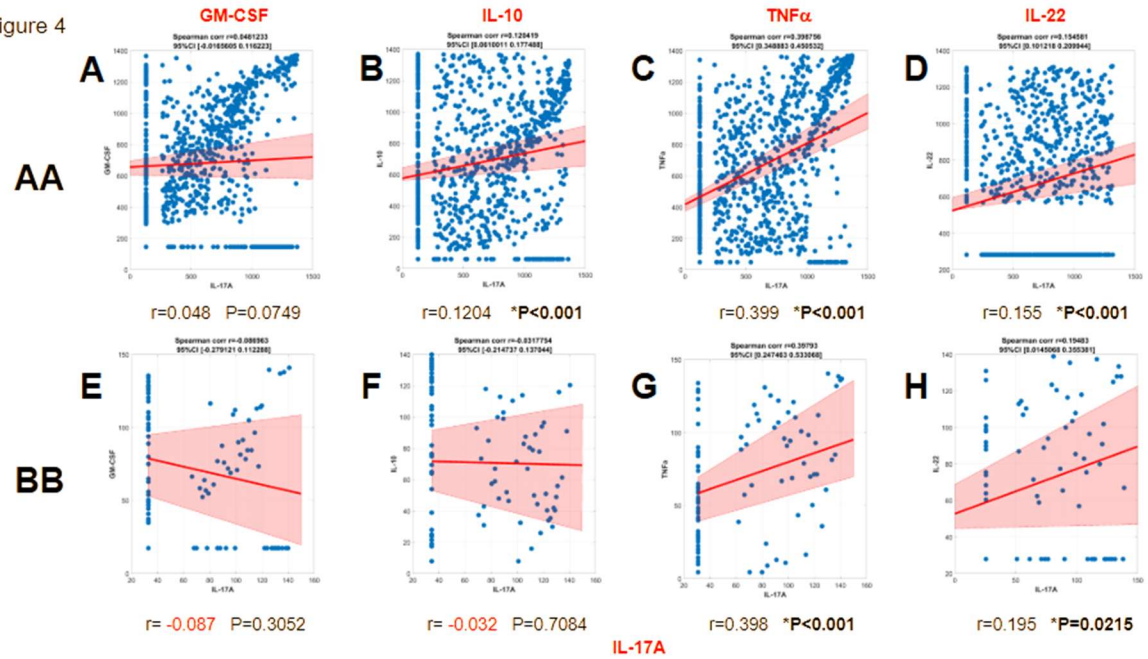
GM-CSF
IL-10
TNFα
IL-22
A
B
C
D
AA
r=0.048 P=0.0749
r=0.1204 *P<0.001
r=0.399 *P<0.001
r=0.155 *P<0.001
E
F
G
H
BB
r= -0.087 P=0.3052
r= -0.032 P=0.7084
r=0.398 *P<0.001
r=0.195 *P=0.0215
IL-17A

Figure 5

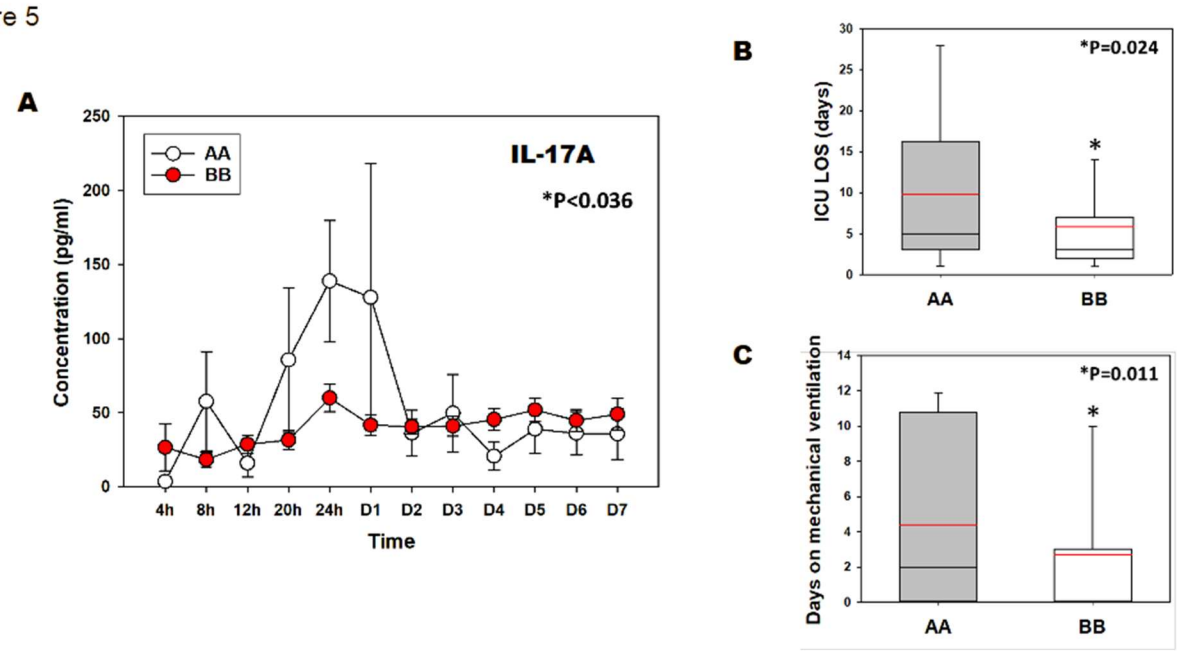
A
IL-17A
*P<0.036
AA
BB
Concentration (pg/ml)
Time
4h
8h
12h
20h
24h
D1
D2
D3
D4
D5
D6
D7
B
*P=0.024
ICU LOS (days)
AA
BB
C
*P=0.011
Days on mechanical ventilation
AA
BB

Figure 6

A

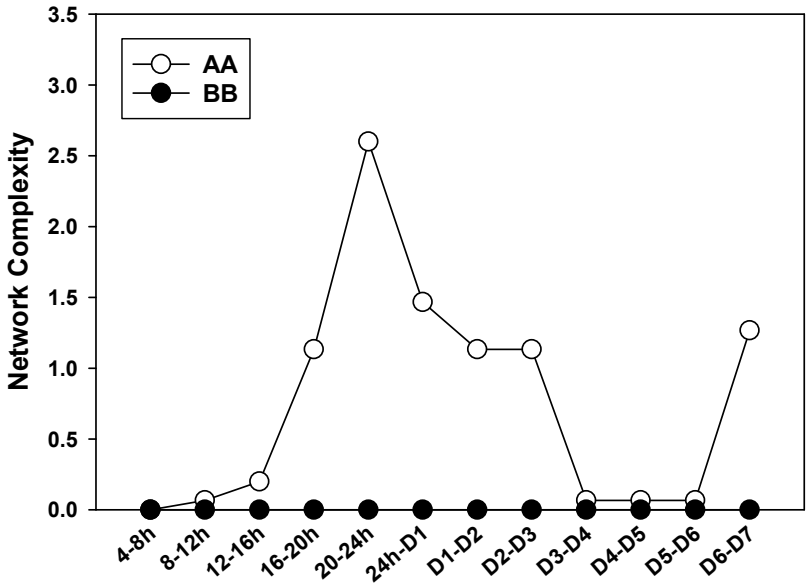

B

Total connectivity	AA 0.95	BB 0.95
IL-5	38	0
IL-7	35	0
IL-2	33	0
IL-15	31	0
IL-1b	24	0
GM-CSF	21	0
IL-1RA	16	0
IL-17A	12	0
IFNg	11	0
IFNa	10	0
IL-4	9	0
MIP-1a	9	0
sIL-2ra	7	0
MIP-1b	5	0
Eotaxin	4	0
IL-22	4	0
IL-33	3	0
IL-17E/IL-25	2	0
IL-8	1	0
IL-21	1	0
IL-6	0	0
IL-9	0	0
IL-10	0	0
IL-13	0	0
IL-23	0	0
IP-10	0	0
MCP-1	0	0
MIG	0	0
NO2-/NO3-	0	0
ST2	0	0
TNFa	0	0

Figure 7

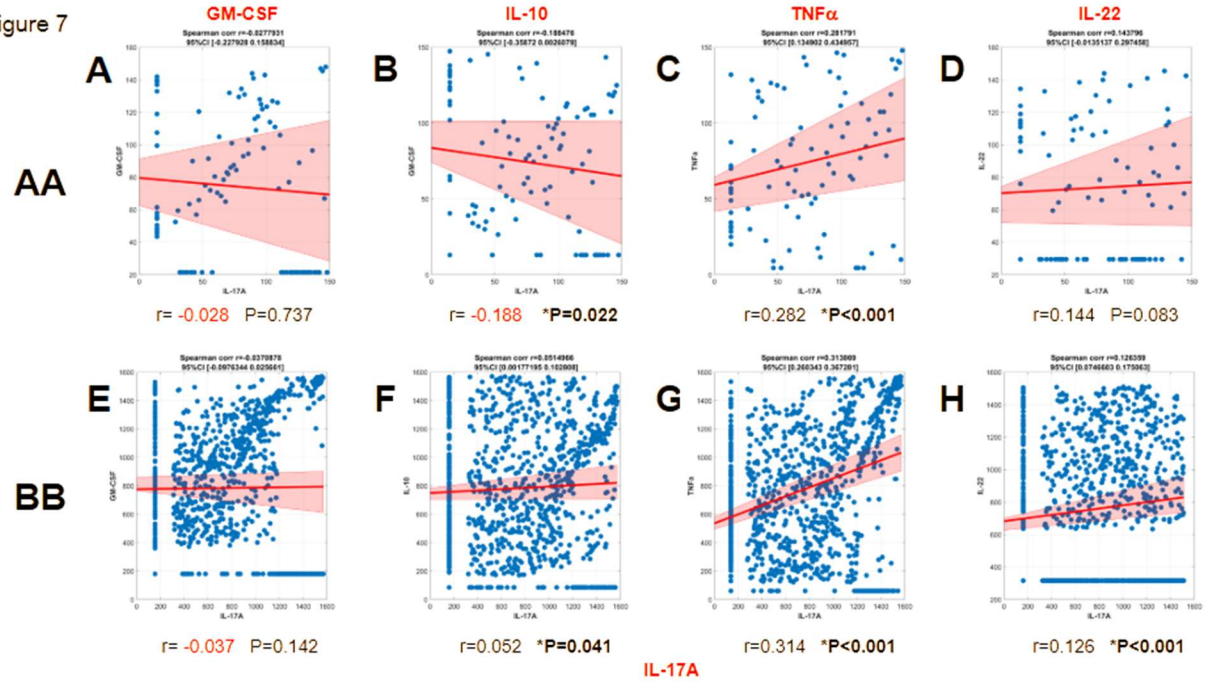
GM-CSF
IL-10
TNFα
IL-22
A
B
C
D
AA
r= -0.028 P=0.737
r= -0.188 *P=0.022
r=0.282 *P<0.001
r=0.144 P=0.083
E
F
G
H
BB
r= -0.037 P=0.142
r=0.052 *P=0.041
r=0.314 *P<0.001
r=0.126 *P<0.001
IL-17A

Figure 8

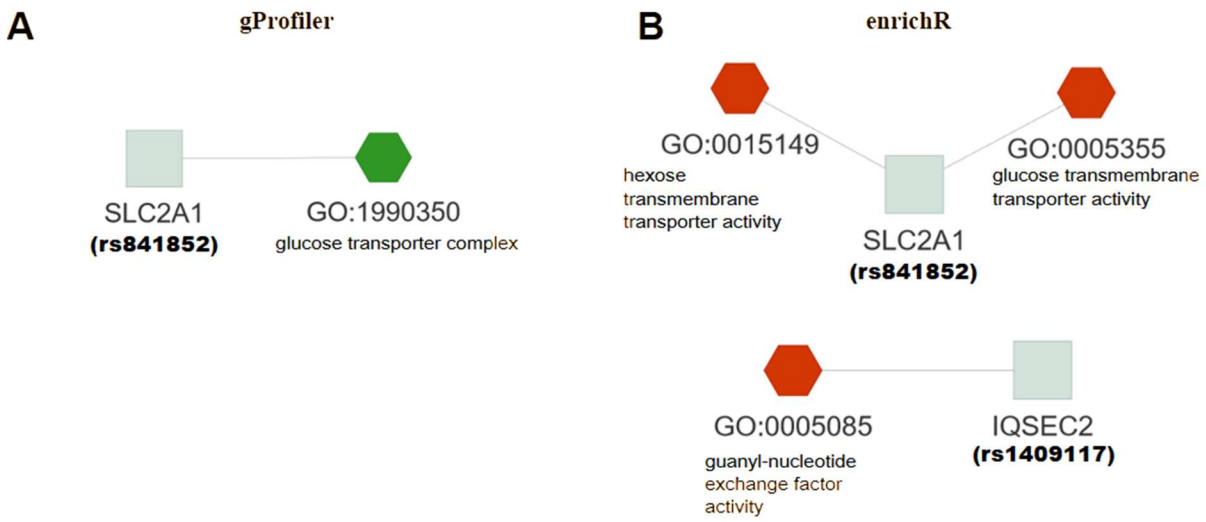
A
gProfiler
SLC2A1
(rs841852)
GO:1990350
glucose transporter complex
B
enrichR
GO:0015149
hexose
transmembrane
transporter activity
GO:0005355
glucose transmembrane
transporter activity
SLC2A1
(rs841852)
GO:0005085
guanyl-nucleotide
exchange factor
activity
IQSEC2
(rs1409117)

Figure 8

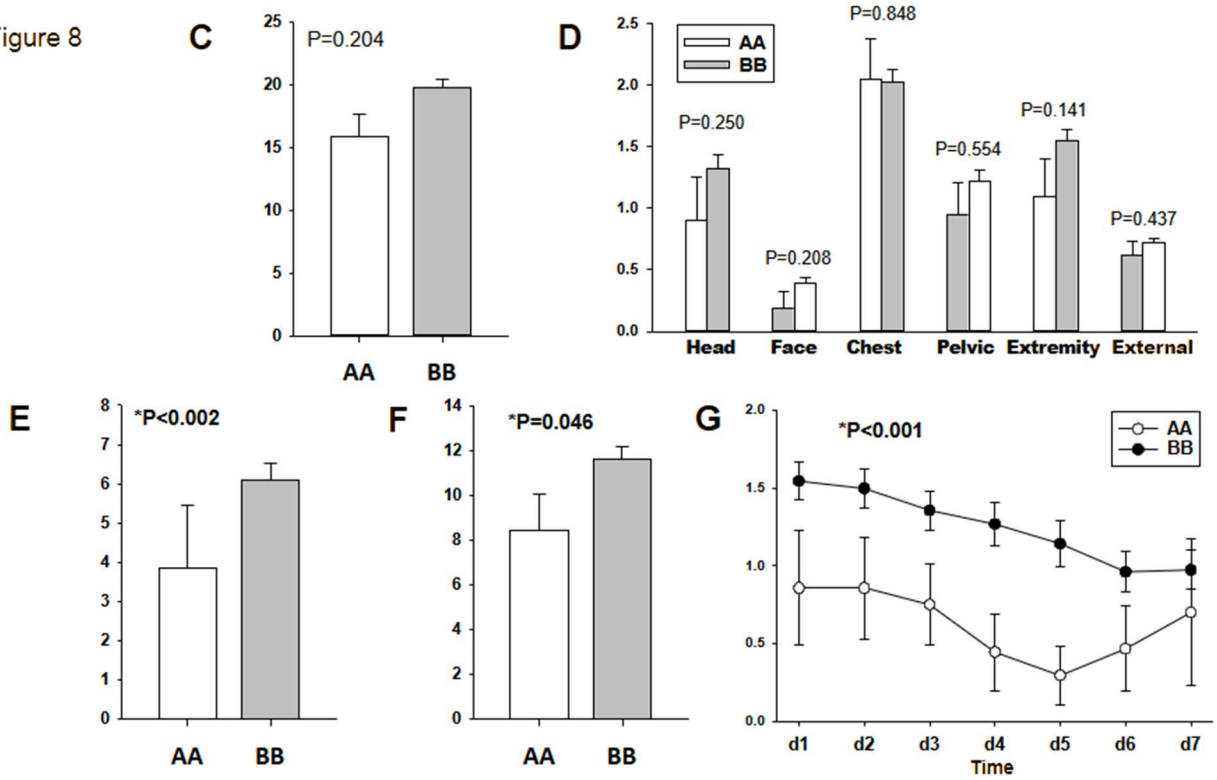
C
P=0.204
AA
BB
D
AA
BB
P=0.250
P=0.208
P=0.848
P=0.554
P=0.141
P=0.437
Head
Face
Chest
Pelvic
Extremity
External
E
*P<0.002
AA
BB
F
*P=0.046
AA
BB
G
*P<0.001
AA
BB
d1
d2
d3
d4
d5
d6
d7
Time

Figure 9

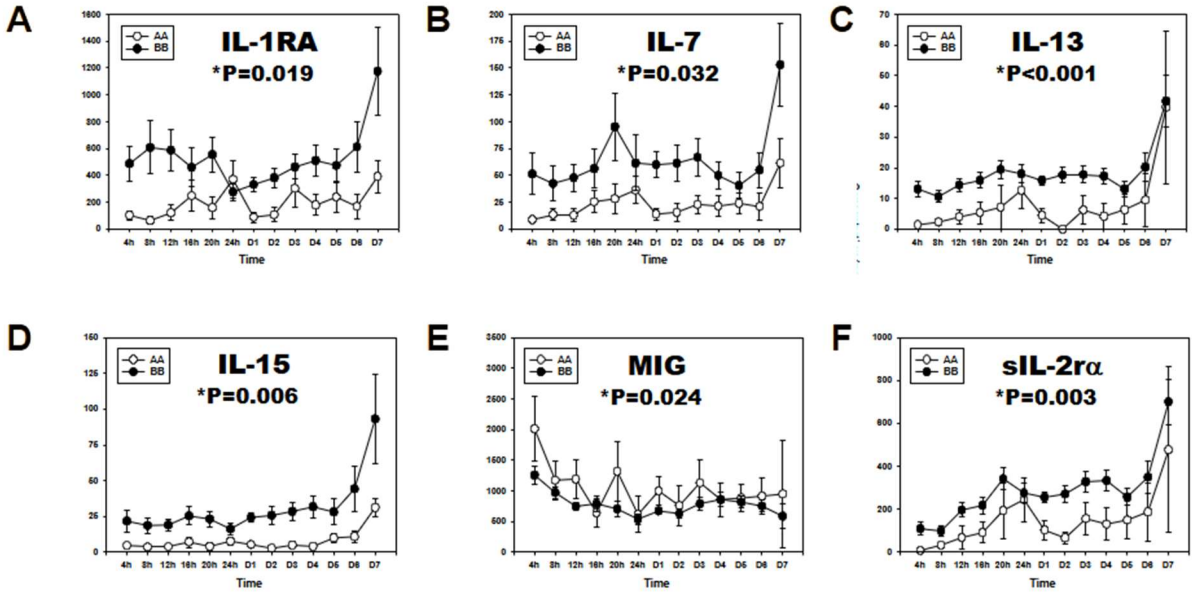
A
IL-1RA
*P=0.019
B
IL-7
*P=0.032
C
IL-13
*P<0.001
D
IL-15
*P=0.006
E
MIG
*P=0.024
F
sIL-2rα
*P=0.003
AA
BB
Time

Figure 10

A

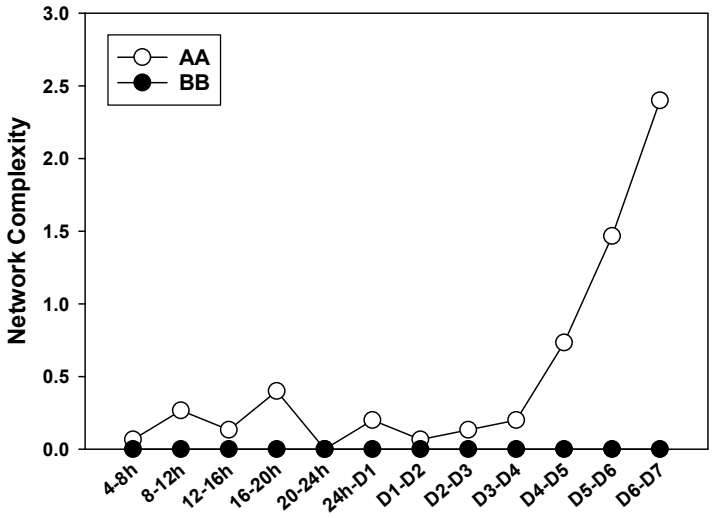

B

Total Connectivity	AA 0.95	BB 0.95
MIP-1a	20	0
IL-4	15	0
IL-5	15	0
IFNg	12	0
IL-7	11	0
IL-13	11	0
IL-17A	11	0
IL-1RA	10	0
IL-33	10	0
IL-1b	9	0
IL-17E/IL-25	9	0
IL-21	9	0
sIL-2ra	9	0
GM-CSF	8	0
IL-22	7	0
IL-23	7	0
IL-2	6	0
IL-10	2	0
MIP-1b	1	0
Eotaxin	0	0
IFNa	0	0
IL-6	0	0
IL-8	0	0
IL-9	0	0
IL-15	0	0
IP-10	0	0
MCP-1	0	0
MIG	0	0
NO2-/NO3-	0	0
ST2	0	0
TNFa	0	0

830

Figure 11

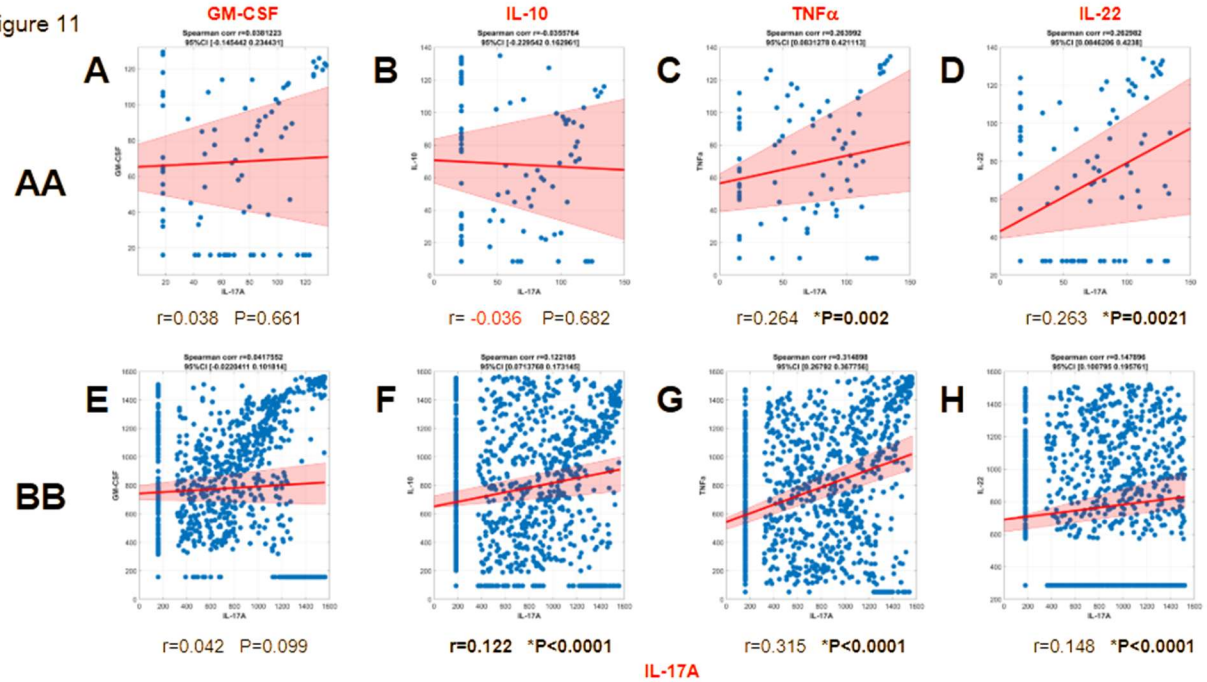

831
832

833 **TABLES**
834
835 Table 1. 'Rare' SNPs entered into FLAME, their number of statistically significant inflammatory
836 biomolecules found by *SNPScanner*, and their corresponding gene/entry found by FLAME (if
837 applicable). (A) SNPs with at least two statistically distinct ($p < 0.00001$) biomolecular
838 differences between AA and BB according to MWU. (B) SNPs with zero statistically distinct (p
839 < 0.05) biomolecular differences.
840

A. 'Rare' Inflammatory Disparity SNPs		
SNP	Number of Distinct Biomolecules ($p < 0.00001$)	Gene/Entry
rs10489239	2	ENSG00000231424
rs6603352	2	KLHL13
rs4774381	2	RORA
rs11782445	2	---
rs7782688	2	---
rs1010779	2	---
rs6603357	2	KLHL13
rs12009735	2	KLHL13
rs6726331	2	LINC01807
rs7258387	2	ENSG00000269110
rs261537	2	UBE2D2
rs13007274	2	FSHR, ENSG00000282890
rs13253492	2	CSMD1
rs7918717	2	RPP38, NMT2
rs11919443	2	TM4SF19, TM4SF19-AS1, TM4SF19-DYNLT2B
B. 'Rare' Control SNPs		
SNP	Number of Distinct Biomolecules ($p < 0.05$)	Gene/Entry
rs1409117	0	IQSEC2
rs2388252	0	ENSG00000235281
rs12450000	0	---
rs4144013	0	PRRG1, ENSG00000250349
rs6609469	0	---
rs9558839	0	---
rs7609779	0	ABI3BP
rs767478	0	---
rs841852	0	SLC2A1
rs7514892	0	RGS21, ENSG00000285280

841

842
843 Table 2. Clinical summary of patients by genotype for rs4774381 (A), rs11919443 (B),
844 rs7918717 (C), rs261537 (D), and rs841852 (E). Parameters marked with an asterisk (*) have
845 five patients with no recorded Shock Index value and four outliers observed in the available
846 patients' data.
847

A. rs4774381 Genotypes			
	AA	AB	BB
Patient Count	223	136	21
Age	50.55 ± 19.08 (min: 18; max: 90)	46.26 ± 18.70 (min: 18; max: 87)	54.90 ± 20.39 (min: 21; max: 85)
Sex			
Male (%)	154 (69.06%)	91 (66.91%)	16 (76.19%)
Female (%)	69 (30.94%)	45 (33.09%)	5 (23.81%)
Ethnicity			
White (%)	220 (98.65%)	130 (95.59%)	18 (85.71%)
African American (%)	1 (0.45%)	6 (4.41%)	3 (14.29%)
Asian (%)	2 (0.90%)	0	0
ISS	19.65 ± 10.32 (min: 1; max: 54)	18.26 ± 10.15 (min: 1; max: 50)	17.38 ± 7.38 (min: 5; max: 30)
ICU Length of Stay (days)	6.51 ± 7.03 (min: 1; max: 36)	5.64 ± 7.10 (min: 1; max: 36)	7.62 ± 8.81 (min: 1; max: 35)
Total Hospital Length of Stay (days)	11.86 ± 9.37 (min: 1; max: 48)	11.44 ± 9.73 (min: 2; max: 50)	13.71 ± 8.11 (min: 2; max: 35)
Days on Mechanical Ventilation	3.26 ± 6.17 (min: 0; max: 34)	2.50 ± 5.74 (min: 0; max: 37)	3.90 ± 6.39 (min: 0; max: 26)
Shock Index*	0.85 ± 0.70 (min: 0.07; max: 8.67)	0.84 ± 0.85 (min: 0.29; max: 9.00)	0.75 ± 0.24 (min: 0.26; max: 1.42)
B. rs11919443 Genotypes			
	AA	AB	BB
Patient Count	20	111	249
Age	57.95 ± 21.10 (min: 23; max: 90)	46.04 ± 17.81 (min: 18; max: 87)	49.99 ± 19.31 (min: 18; max: 89)
Sex			
Male (%)	14 (70%)	88 (79.28%)	159 (63.86%)
Female (%)	6 (30%)	23 (20.72%)	90 (36.14%)
Ethnicity			

White (%)	18 (90%)	108 (97.30%)	242 (97.19%)
African American (%)	1 (5%)	2 (1.80%)	7 (2.81%)
Asian (%)	1 (5%)	1 (0.90%)	0
ISS	18.35 ± 10.23 (min: 5; max: 48)	20.06 ± 10.91 (min: 1; max: 54)	18.62 ± 9.75 (min: 1; max: 50)
ICU Length of Stay (days)	9.85 ± 9.02 (min: 1; max: 33)	6.57 ± 7.91 (min: 1; max: 36)	5.83 ± 6.56 (min: 1; max: 36)
Total Hospital Length of Stay (days)	16.40 ± 13.04 (min: 2; max: 48)	12.63 ± 9.54 (min: 1; max: 45)	11.08 ± 8.92 (min: 2; max: 50)
Days on Mechanical Ventilation	4.40 ± 4.47 (min: 0; max: 14)	3.50 ± 7.54 (min: 0; max: 37)	2.70 ± 5.31 (min: 0; max: 28)
Shock Index*	0.68 ± 0.15 (min: 0.49; max: 1.04)	0.87 ± 0.81 (min: 0.07; max: 8.67)	0.84 ± 0.74 (min: 0.30; max: 9.00)
C. rs7918717 Genotypes			
	AA	AB	BB
Patient Count	242	117	21
Age	49.78 ± 19.15 (min: 18; max: 90)	46.76 ± 18.79 (min: 18; max: 86)	57.10 ± 19.06 (min: 20; max: 83)
Sex			
Male (%)	168 (69.42%)	78 (66.67%)	15 (71.43%)
Female (%)	74 (30.58%)	29 (24.79%)	6 (28.57%)
Ethnicity			
White (%)	239 (98.76%)	114 (97.44%)	15 (71.43%)
African American (%)	1 (0.41%)	3 (2.56%)	6 (28.57%)
Asian (%)	2 (0.82%)	0	0
ISS	18.70 ± 10.00 (min: 1; max: 50)	19.40 ± 10.35 (min: 1; max: 54)	20.71 ± 10.48 (min: 4; max: 50)
ICU Length of Stay (days)	5.73 ± 6.69 (min: 1; max: 33)	7.00 ± 7.72 (min: 1; max: 36)	8.19 ± 8.70 (min: 1; max: 35)
Total Hospital Length of Stay (days)	11.15 ± 8.84 (min: 1; max: 50)	13.30 ± 10.67 (min: 2; max: 46)	11.19 ± 7.95 (min: 2; max: 35)
Days on Mechanical Ventilation	2.59 ± 5.28 (min: 0; max: 27)	3.74 ± 7.41 (min: 0; max: 37)	3.95 ± 5.40 (min: 0; max: 17)
Shock Index*	0.82 ± 0.75 (min: 0.07; max: 9.00)	0.89 ± 0.79 (min: 0.38; max: 8.67)	0.73 ± 0.22 (min: 0.41; max: 1.22)
D. rs261537 Genotypes			

	AA	AB	BB
Patient Count	223	136	21
Age	49.47 ± 19.19 (min: 18; max: 86)	48.20 ± 19.11 (min: 18; max: 90)	53.86 ± 18.72 (min: 23; max: 85)
Sex			
Male (%)	154 (69.06%)	91 (66.91%)	16 (76.19%)
Female (%)	69 (30.94%)	45 (33.09%)	5 (23.81%)
Ethnicity			
White (%)	219 (98.2%)	130 (95.59%)	19 (90.48%)
African American (%)	2 (0.90%)	6 (4.41%)	2 (9.52%)
Asian (%)	2 (0.90%)	0	0
ISS	18.53 ± 10.23 (min: 1; max: 54)	20.15 ± 10.20 (min: 4; max: 50)	17.86 ± 8.28 (min: 5; max: 42)
ICU Length of Stay (days)	6.24 ± 7.18 (min: 1; max: 36)	6.62 ± 7.41 (min: 1; max: 35)	4.14 ± 5.05 (min: 1; max: 24)
Total Hospital Length of Stay (days)	11.97 ± 10.00 (min: 2; max: 50)	11.76 ± 8.79 (min: 1; max: 45)	10.48 ± 7.15 (min: 2; max: 33)
Days on Mechanical Ventilation	2.91 ± 5.80 (min: 0; max: 34)	3.43 ± 6.66 (min: 0; max: 37)	1.67 ± 3.68 (min: 0; max: 17)
Shock Index*	0.86 ± 0.70 (min: 0.30; max: 9.00)	0.83 ± 0.85 (min: 0.07; max: 8.67)	0.68 ± 0.19 (min: 0.30; max: 0.99)
E. rs841852 Genotypes			
	AA	AB	BB
Patient Count	21	109	250
Age	57.90 ± 15.83 (min: 23; max: 85)	49.59 ± 19.25 (min: 18; max: 87)	48.38 ± 19.22 (min: 18; max: 90)
Sex			
Male (%)	12 (57.14%)	80 (73.39%)	169 (67.60%)
Female (%)	9 (42.86%)	29 (26.61%)	81 (32.40%)
Ethnicity			
White (%)	19 (90.48%)	104 (95.41%)	245 (98.00%)
African American (%)	2 (9.52%)	5 (4.59%)	3 (1.20%)
Asian (%)	0	0	2 (0.80%)
ISS	15.86 ± 7.83 (min: 1; max: 30)	17.93 ± 10.23 (min: 1; max: 50)	19.77 ± 10.19 (min: 1; max: 54)
ICU Length of Stay	3.86 ± 7.19	7.12 ± 7.86	6.08 ± 6.81

(days)	(min: 1; max: 35)	(min: 1; max: 33)	(min: 1; max: 36)
Total Hospital Length of Stay (days)	8.43 ± 7.20 (min: 2; max: 35)	12.96 ± 10.24 (min: 2; max: 48)	11.60 ± 9.17 (min: 1; max: 50)
Days on Mechanical Ventilation	1.00 ± 2.58 (min: 0; max: 12)	3.58 ± 6.31 (min: 0; max: 31)	2.95 ± 6.10 (min: 0; max: 37)
Shock Index*	1.02 ± 1.80 (min: 0.07; max: 9.00)	0.88 ± 0.94 (min: 0.42; max: 8.67)	0.81 ± 0.42 (min: 0.26; max: 5.4)

848